การรีฟอร์มมิ่งด้วยคาร์บอนไดออกไซด์ของมีเทน ภายใต้การดำเนินงานแบบสับเปลี่ยนการป้อน

นาย เอกพล พรหมรส

CARBON DIOXIDE REFORMING OF METHANE UNDER PERIODIC OPERATION
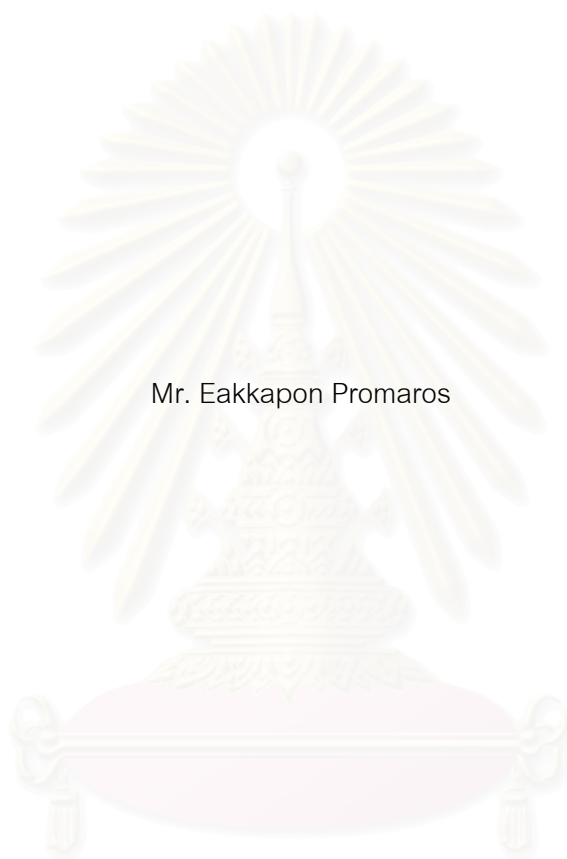
Mr. Eakkapon Promaros

A Thesis Submitted in Partial Fulfillment of the Requirements

for the Degree of Master of Engineering Program in Chemical Engineering

Department of Chemical Engineering

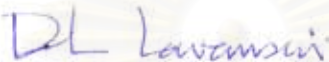Faculty of Engineering

Chulalongkorn University

Academic Year 2005

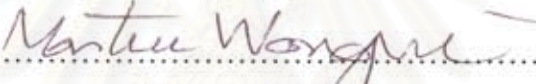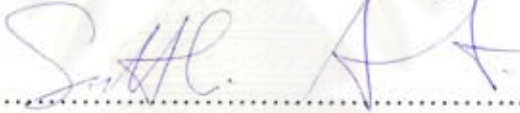| Thesis Title | CARBON DIOXIDE REFORMING OF METHANE UNDER PERIODIC OPERATION |
|---|---|
| By | Mr. Eakkapon Promaros |
| Field of Study | Chemical Engineering |
| Thesis Advisor | Associate Professor Suttichai Assabumrungrat, Ph.D. |
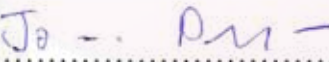
Accepted by the Faculty of Engineering, Chulalongkorn University in Partial Fulfillment of the Requirements for the Master's Degree

.......................................Dean of the Faculty of Engineering

(Professor Direk Lavansiri, Ph.D.)

THESIS COMMITTEE

.......................................... Chairman

(Assistant Professor Montree Wongsri, D.Sc.)

........................................... Thesis Advisor

(Associate Professor Suttichai Assabumrungrat, Ph.D.)

............................................... Member

(Assistant Professor Joongjai Panpranot, Ph.D.)

............................................... Member

(Assistant Professor Muenduen Phisalaphong, Ph.D.)

เอกพล พรหมรส: การรีฟอร์มมิ่งด้วยคาร์บอนไดออกไซด์ของมีเทนภายใต้การดำเนินงานแบบสับเปลี่ยนการป้อน (CARBON DIOXIDE REFORMING OF METHANE UNDER PERIODIC OPERATION) อ. ที่ปรึกษา : รศ.ดร.สุทธิชัย อัสสะบำรุงรัตน์, 69 หน้า. ISBN 974-17-5913-4

งานวิจัยนี้ทำการศึกษาปฏิกิริยาการรีฟอร์มมิ่งด้วยคาร์บอนไดออกไซด์ของมีเทน บนตัวเร่งปฏิกิริยาโลหะนิกเกิลบนตัวรองรับซิลิกาออกไซด์และแมกนีเซียมออกไซด์ที่ใช้งานอย่างแพร่หลายในอุตสาหกรรม ปฏิกิริยานี้เป็นการใช้ประโยชน์จากก๊าซคาร์บอนไดออกไซด์และมีเทนซึ่งเป็นส่วนประกอบหลักในก๊าซธรรมชาติและก๊าซชีวภาพ ในการผลิตก๊าซสังเคราะห์ที่มีอัตราส่วนของไฮโดรเจนเทียบกับคาร์บอนมอนออกไซด์ต่ำได้อย่างมีประสิทธิภาพ โดยงานวิจัยนี้มีเป้าหมายในการศึกษาความเป็นได้ที่จะนำระบบการดำเนินงานแบบสับเปลี่ยนการป้อนมาปรับใช้กับปฏิกิริยาดังกล่าว ซึ่งในการดำเนินงาน มีเทนจะถูกป้อนเข้าไปเพื่อให้เกิดปฏิกิริยาการแตกตัวของมีเทนซึ่งจะได้ก๊าซไฮโดรเจนและคาร์บอนซึ่งจะสะสมตัวอยู่บนตัวเร่งปฏิกิริยา จากนั้นตัวเร่งปฏิกิริยาจะถูกคืนสภาพด้วยการป้อนคาร์บอนไดออกไซด์เพื่อให้เกิดปฏิกิริยาออกซิเดชันกับคาร์บอนที่สะสมอยู่ ผลของตัวแปรต่างๆ เช่น ระยะเวลาการสับเปลี่ยนสารตั้งต้น อัตราส่วนของระยะเวลาในการสับเปลี่ยน และอุณหภูมิในการเกิดปฏิกิริยาในการดำเนินการแบบสับเปลี่ยนการป้อน จะถูกนำมาเปรียบเทียบกับระการดำเนินการแบบไหลร่วม โดยที่อัตราการป้อนเฉลี่ยของสารตั้งต้นทั้งสองชนิดจะถูกควบคุมให้เท่ากันในทุกกรณี ซึ่งค่าการเปลี่ยนของมีเทนและค่าร้อยละของผลได้ของไฮโดรเจนที่อุณหภูมิ 1023 องศาเคลวิน จะค่อยๆลดลงตามเวลาจนกระทั่งคงตัวอยู่ที่ประมาณครึ่งหนึ่งของค่าที่ได้จากการดำเนินงานแบบไหลร่วม ทั้งนี้เนื่องมาจากการสะสมตัวของคาร์บอนและการสูญเสียตำแหน่งว่องไวของตัวเร่งปฏิกิริยา ซึ่งแตกต่างจากที่อุณหภูมิ 923 องศาเคลวิน ค่าการเปลี่ยนของมีเทนและค่าร้อยละของผลได้ของไฮโดรเจนจะไม่มีการเปลี่ยนแปลงไปตามเวลา แม้ว่าจะมีการสะสมตัวของคาร์บอนระหว่างปฏิกิริยามากกว่าก็ตาม โดยที่อุณหภูมิดังกล่าว ค่าร้อยละของผลได้ของไฮโดรเจนจากทั้งสองระบบก็ยังมีค่าใกล้เคียงกันอีกด้วย สาเหตุของพฤติกรรมเหล่านี้ อาจเกิดจากกลไกการเกิดคาร์บอนบนตัวเร่งปฏิกิริยาที่แตกต่างกันที่อุณหภูมิต่างกัน ซึ่งควรมีการศึกษาเพิ่มเติมเพื่อให้ทราบถึงของสาเหตุที่แท้จริงต่อไปในอนาคต นอกจากนี้ จากการวิจัยยังพบว่า การเปลี่ยนแปลงระยะเวลาการสับเปลี่ยนสารตั้งต้นและอัตราส่วนของระยะเวลาในการสับเปลี่ยนไม่ได้ส่งผลอย่างชัดเจนต่อประสิทธิภาพของระบบการดำเนินงานแบบกะภายใต้ขอบเขตของงานวิจัย

ภาควิชา...............วิศวกรรมเคมี........... ลายมือชื่อนิสิต.......................................

สาขาวิชา...............วิศวกรรมเคมี........... ลายมือชื่ออาจารย์ที่ปรึกษา.......................

ปีการศึกษา...........2548...................

##4770549521: MAJOR CHEMICAL ENGINEERING

KEY WORD: CARBON DIOXIDE REFORMING OF METHANE/ NICKEL/ CARBONACEOUS DEPOSITION/ PERIODIC OPERATION

EAKKAPON PROMAROS: CARBON DIOXIDE REFORMING OF METHANE UNDER PERIODIC OPERATION. THESIS ADVISOR: ASSOC.PROF. SUTTICHAI ASSABUMRUNGRAT, Ph.D. 69 pp. ISBN: 974-17-5913-4

This work investigates the carbon dioxide reforming of methane on a commercial $Ni/SiO_2.MgO$ catalyst. Methane and carbon dioxide, which are major components found in natural gas and biogas, are efficiently utilized for the production of synthesis gas with low $H_2/CO$ ratio. The study is aimed at investigating the possibility for applying the periodic operation to this reaction. In the operation, pure methane was fed to the catalyst bed where the methane cracking reaction took place, yielding hydrogen and carbonaceous deposit. The catalyst was regenerated via the reverse Boudouard reaction under a flow of pure carbon dioxide. The effect of key parameters such as cycle period, cycle split, and reaction temperature were investigated and the results were compared with those from the steady state operation. All experiments were carried out under the same time-average flow rate of both reactants. At 1023 K, the methane conversion and hydrogen yield initially decreased with time on stream and eventually leveled off, giving the values about half of those from the steady state operation. The decreased catalytic activity was due to the accumulation of carbonaceous deposit and loss of metal active sites. The different trend was observed at 923 K. The methane conversion and hydrogen yield were not changed with the time on stream although more carbonaceous deposit was accumulated during the reaction course. At this temperature, the periodic operation offered the equivalent hydrogen yield to the steady state operation. The observed behavior may be due to the different mechanisms of carbon formation over the catalyst. Further investigations are required to elucidate this unusual behavior. Finally it was found that no significant effects of cycle period and cycle spilt on the reaction performance was observed at least within the ranges of this study.

Department......Chemical Engineering...    Student's signature...................

Field of study...Chemical Engineering...    Advisor's signature...................

Academic year.....2005....................

# ACKNOWLEDGEMENTS

# CONTENTS

# LIST OF TABLES

# LIST OF FIGURES

# NOMENCLATURE

| | | |
|---|---|---|
| $s$ | Cycle split, duty fraction | [-] |
| $A_i$ | Amplitude of $i$ | [various units] |
| $x_i$ | Conversion of $I$ | [%] |

**Greeks letters**

| | | |
|---|---|---|
| $\tau$ | Cycle or forcing period | [min] |

# CHAPTER I
# INTRODUCTION

## 1.1 Rational

There are many methods for producing hydrogen and synthesis gas. Steam reforming of hydrocarbons particularly methane is widely used and generally considered as the most economical ways to produce hydrogen and synthesis gas products. Carbon dioxide reforming of methane is currently an attractive process which shows a growing interest from both industrial and environmental viewpoints.

From an environmental perspective, natural gas found in Southeast Asia contains a large amount of carbon dioxide ($CO_2$). It remains not widely used due to high $CO_2$ content. Methane ($CH_4$) can also be produced through anaerobic biomass fermentation of industrial waste water, and $CO_2$ still appears as a major co-product of this process. Both $CH_4$ and $CO_2$ are major greenhouse gases causing the global warming problem. They can be consumed by the carbon dioxide reforming reaction.

$$CH_4 + CO_2 \rightarrow 2CO + 2H_2 \qquad (1.1)$$
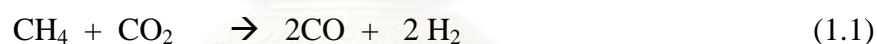
From the industrial point of view, the reaction allows to transform these gases into synthesis gas with a low $H_2/CO$ ratio, adequate for hydroformylation and carbonylation reactions as well as for methanol, oxygenated compounds and Fischer–Tropsch syntheses.

Several supported transition metal catalysts (Ni, Ru, Rh, Pd, etc.) have been investigated for the carbon dioxide reforming of methane (Fischer and Tropsch., 1928; Gadalla *et al*., 1988; Rostrup-Nielsen *et al*., 1993). Nickel catalysts are mainly used in industry due to their low cost. A typical problem found in this catalytic reaction is catalyst deactivation. The carbonaceous deposition in the reactor is mainly generated from the following catalytic cracking of methane.

$$CH_4 \rightarrow C + 2H_2 \qquad (1.2)$$

However, the presence of carbon dioxide helps remove the deposited carbon according to the following reverse Boudouard reaction (Takano *et al*., 1996).

$$C + CO_2 \rightarrow 2CO \hspace{3cm} (1.3)$$

As shown in the above equations (Eqs. 1.2 and 1.3), the carbon dioxide reforming of methane (Eq. 1.1) can be operated periodically by feeding methane and carbon dioxide alternately as illustrated in Figure 1.1. Under this operation, the products, hydrogen and carbon monoxide, appear at different time and therefore the direct separation of the products can be obtained without further significant effort. Therefore, this operation is attractive particularly for the case when carbon monoxide-free hydrogen is required for some applications like in proton-exchange membrane (PEM) fuel cell. In addition, the advantage in periodic operation of the reaction can be gained from heat coupling of endothermic methane cracking and exothermic carbon oxidation. In practice, it could be, for example, a coaxial reactor operated periodically, so that the heat released during the carbon oxidation can be used in situ for the reaction of cracking methane. Although the periodic operation for this reaction is conceptually attractive, there is still no effort to demonstrate experimentally the benefit of the operation.

In this work, the periodic operation for the carbon dioxide reforming of methane is investigated. The operation involves two steps of

1) methane decomposition reaction over industrial steam reforming Ni/SiO$_2$.MgO catalyst, and
2) catalyst regeneration via oxidation of the deposited carbon with carbon dioxide mixture.

The effects of operating variables of periodic operation like period time, cycle split and operating temperature on conversions of methane and carbon dioxide, and selectivity and yield of hydrogen are investigated and compared with the results from steady state operation.
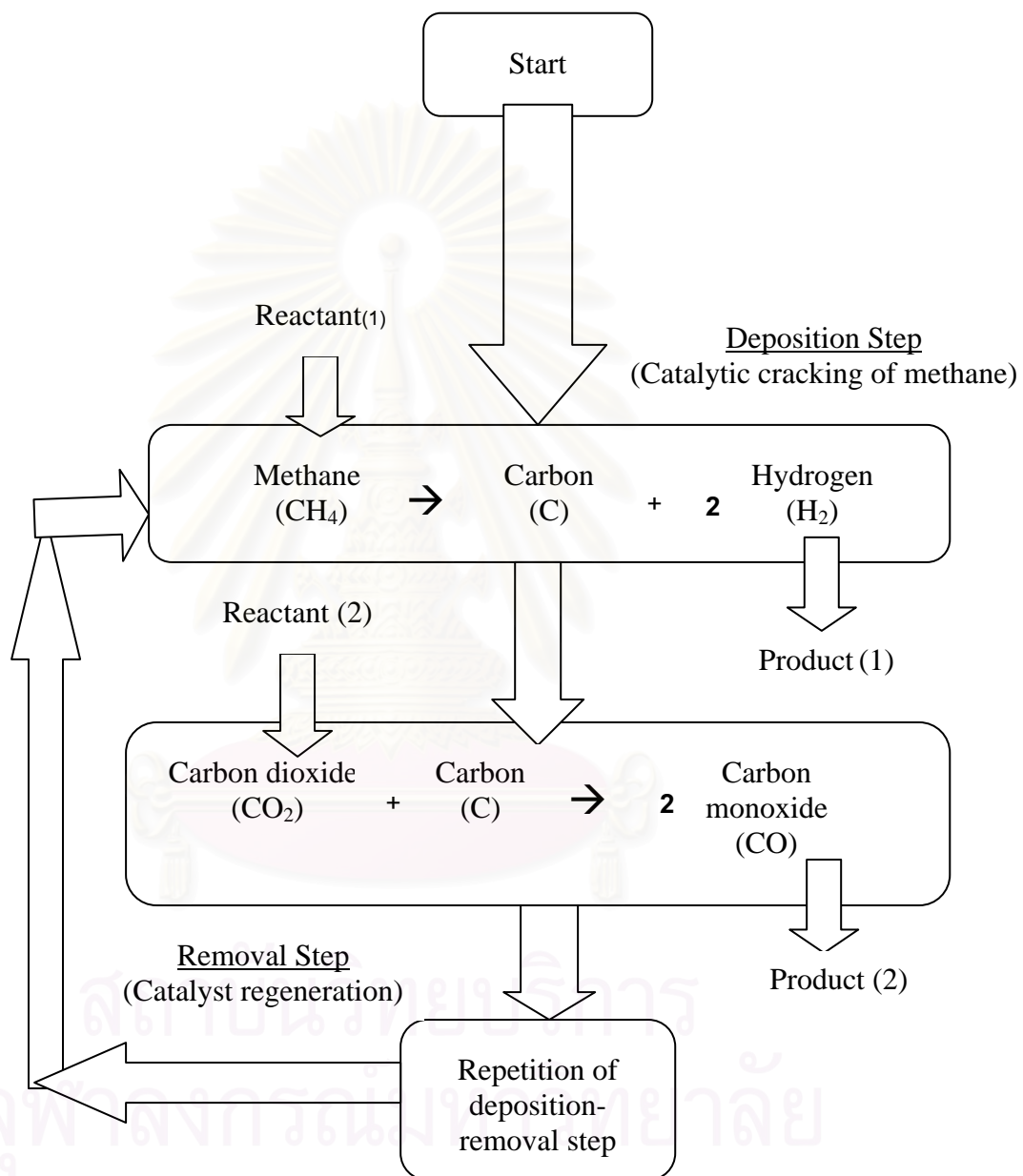
**Figure 1.1** Periodic operation of carbon dioxide reforming of methane

## 1.2 Objectives

The objectives of this research can be summarized as follows:

1) To investigate the performance of the periodic operation for the carbon dioxide reforming of methane over $Ni/SiO_2.MgO$, an industrial steam reforming catalyst, compared with the steady state operation.

2) To study the effect of operating parameters such as reaction temperature, duration of length and cycle split ratio of cracking/regeneration period on the performance of the reactor.

## 1.3 Thesis Organization

This present work is organized as follows:

The rational and objectives of the work are described in Chapter I.

The theory of this research, i.e. studies about the carbon dioxide reforming of methane reaction and its possible mechanisms, and the periodic operation are presented in Chapter II.

Chapter III reviews research works on the carbon dioxide reforming of methane reaction, catalytic cracking of methane and catalyst regeneration in the past and comments on previous works.

Chapter IV consists of method and process for studying reaction in this research.

The experimental results and discussion are described in Chapter V.

Chapter VI contains the overall conclusion observed from this work and some recommendations for future work.

Finally, the sample of calculation for conversion, calibration curves from area to mole of product, and reactant gases, and the experimental data are included in appendices at the end of this thesis.

# CHAPTER II
# THEORY

## 2.1 Reforming reaction

There are three main processes for producing hydrogen and synthesis gas from methane as follows.

- Steam reforming

$$CH_4 + H_2O \quad \rightarrow \quad CO + 3H_2 \qquad \Delta H = 208 \, kJ/mol \qquad \text{(i)}$$

- Carbon dioxide reforming

$$CH_4 + CO_2 \quad \rightarrow \quad 2CO + 2H_2 \qquad \Delta H = 248 \, kJ/mol \qquad \text{(ii)}$$

- Partial oxidation

$$CH_4 + \frac{1}{2}O_2 \quad \rightarrow \quad CO + 2H_2 \qquad \Delta H = -36 \, kJ/mol \qquad \text{(iii)}$$
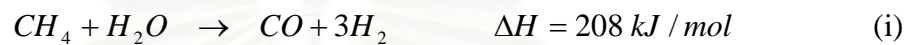
Steam reforming of methane is widely industrialized as a method of synthesis gas production. However at present time, because reduction of green house gases such as $CO_2$ and $CH_4$ is of great concern, effective utilization of both gases are required from a global environmental view point. Moreover, synthesis gas, produced from $CO_2$ reforming process, has low $H_2/CO$ ratio which is effective for the synthesis of valuable oxygenated chemicals and for the Fischer-Tropsch synthesis of higher hydrocarbons. Therefore, $CO_2$ reforming of $CH_4$ is the reaction of interest in this study.

### 2.1.1 Thermodynamics of carbon dioxide reforming of methane

The reforming of methane with carbon dioxide (Eq. 2.1) is a highly endothermic reaction, which has similar thermodynamic and equilibrium characteristics to steam reforming reaction (Eq. 2.2). However, the produced synthesis gas has a lower $H_2/CO$ ratio.

$$CH_4 + CO_2 \quad \rightarrow \quad 2CO + 2H_2 \qquad \Delta H = 248 \, kJ/mol \qquad (2.1)$$

$$CH_4 + H_2O \quad \rightarrow \quad CO + 3H_2 \qquad \Delta H = 208 \, kJ/mol \qquad (2.2)$$

Similar to the steam reforming, the carbon dioxide reforming of methane is likely to be conducted under conditions where carbon formation via catalytic cracking of methane (Eq. 2.3) and/or Boudouard reaction (Eq. 2.4) is thermodynamically feasible.

$$CH_4 \quad \rightarrow \quad C + 2H_2 \qquad \Delta H = 75 \, kJ/mol \qquad (2.3)$$

$$2CO \quad \rightarrow \quad C + CO_2 \qquad \Delta H = -171 \, kJ/mol \qquad (2.4)$$
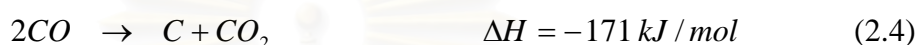
Other reactions which could also have an important influence on the overall product spectrum are:

$$CO_2 + H_2 \quad \rightarrow \quad CO + H_2O \qquad \Delta H = 40 \, kJ/mol \qquad (2.5)$$

$$C + H_2O \quad \rightarrow \quad CO + H_2 \qquad \Delta H = 131 \, kJ/mol \qquad (2.6)$$

Thus, in carbon dioxide reforming of methane, the cracking of methane (Eq. 2.3) and the reverse of reaction (2.4) also take place. Theoretically, the carbon formed in reaction (2.3) should be rapidly consumed by the reverse of reaction (2.4), and by the steam/carbon gasification reaction (i.e., reaction (2.6)).

Reaction (2.6) can play a role in carbon dioxide reforming of methane because steam is almost always formed via the reverse water gas-shift (RWGS) reaction (Eq. 2.5). If reaction (2.3) is faster than the carbon removal rate, there is a net build-up of carbon to pose serious problems in the overall reaction. The formation of solid carbon leads to catalyst deactivation and plugging problem in the reactor.

It should be noted that the formation of water is not desired in this reaction system as it decreases the selectivity of hydrogen.

### 2.1.2 Reaction mechanism carbon dioxide reforming of methane

Attempts to clarify the reaction mechanism in the carbon dioxide reforming of methane have been investigated in many researches. Solymosi *et al.* (1991, 1993) proposed the possible mechanism of carbon dioxide reforming of methane reaction over supported metal catalyst. Activation of methane would be produced via dissociation of methane with activation carbon formed at the end of reaction as followed;

$$CH_4 \quad \rightarrow \quad CH_3^* + H^*, \tag{2.3a}$$

$$CH_3^* \quad \rightarrow \quad CH_2^* + H^*, \tag{2.3b}$$

$$CH_2^* \quad \rightarrow \quad CH^* + H^*, \tag{2.3c}$$

$$CH^* \quad \rightarrow \quad C^* + H^*. \tag{2.3d}$$
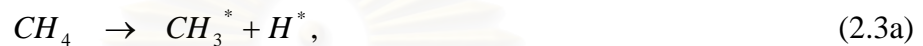
When carbonaceous deposition is formed on the catalyst surface, it blocks the active site and hinders dissociation of methane. Generally, the carbon deposits may have many forms which are different in terms of reactivity: adsorbed atomic carbon (highly reactive form), amorphous carbon, vermicular carbon, bulk nickel carbide, and crystalline graphitic carbon. The reactivity of carbon deposit depends on the type of catalyst surface, the temperature of its formation and the duration of thermal treatment. This would be considered to carbon formed from carbon monoxide as the precursor as shown by Eq. (2.7b).

$$CO_2 \quad \rightarrow \quad CO^* + O^*, \tag{2.7a}$$

$$CO^* \quad \rightarrow \quad C^* + O^*. \tag{2.7b}$$

Unless both methane and carbon dioxide dissociate separately, their deposited products terminate the respective dissociation by covering the metal surfaces. The self-decomposition of both methane and carbon dioxide could be facilitated via reactions (2.8)-(2.10). The dissociation of methane is enhanced by adsorbed oxygen, while the dissociation of carbon dioxide is also promoted by adsorbed hydrogen and

other methane residues. Therefore, the reactions of these surface species also need to be considered as the following reactions:

$$CO_2 + H^* \quad \rightarrow \quad CO^* + OH^*, \tag{2.8}$$

$$CH_4 + O^* \quad \rightarrow \quad CH_3^* + OH^*, \tag{2.9}$$

$$CH_x + O^* \quad \rightarrow \quad CO + xH^*, \tag{2.10}$$

$$2OH^* \quad \rightarrow \quad H_2O + O^*. \tag{2.11}$$

### 2.1.3 Mechanism of Carbon Formation

Carbon formation on catalysts is an important problem in many processes such as steam reforming and methanation, and also in carbon dioxide reforming of methane. Coke formation may cause deactivation of the catalyst surface, blocking of catalyst pores and voids, or also physical properties of the catalyst support.

During the reaction, various types of carbon may be formed. In case of carbon dioxide reforming of methane over nickel catalyst, two main types of deposited carbon were indicated to be formed, encapsulate and whisker carbons. Figure 2.1 shows the mechanism of carbon formation which has been constructed on the basis of following steam reforming mechanism;

$$CO_2 \quad \rightarrow \quad CO + O_{Ad-metal} \tag{i}$$

$$CO_2 \quad \rightarrow \quad CO + O_{Ad-\text{sup }port} \tag{ii}$$

$$CH_4 \quad \rightarrow \quad CH_{x-metal} + (4-x)/2H_2 \tag{iii}$$

$$CH_{x-metal} + O_{Ad-metal} \rightarrow \quad x/2H_2 + CO \tag{iv}$$

$$CH_{x-metal} + O_{Ad-\text{sup }portl} \rightarrow \quad x/2H_2 + CO \tag{v}$$
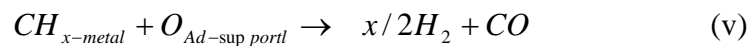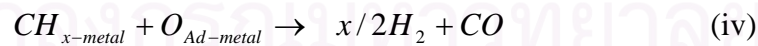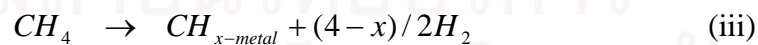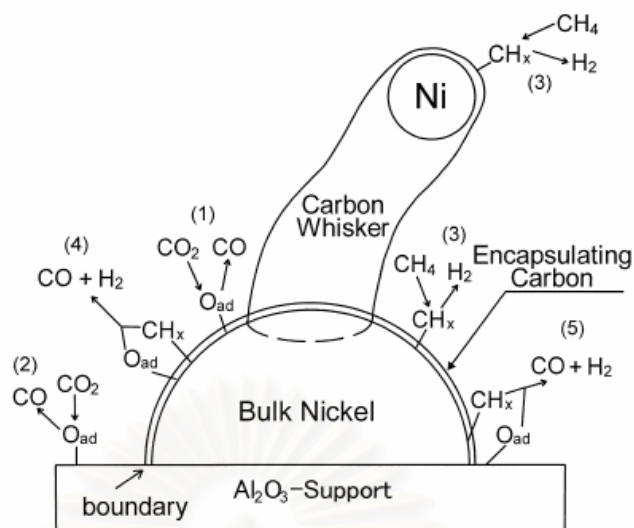
**Figure 2.1** Model of reforming reaction and carbonaceous reaction (Ito,1999)

Two types of active sites were proposed on the catalyst, the one interacted with the catalyst support, the other at the surface of bulk nickel. The former mainly participated in the reforming reaction while the latter was involved with carbonaceous deposition. Carbon deposited on the surface of bulk nickel is assembled to form carbon whiskers with nickel growing on top. If the nickel in the growing core can only be removed, carbonaceous deposition is suppressed without any deactivation of reforming activity because the nickel interacted with support which mainly participates in the reforming reaction is not detached.

For the catalytic cracking of methane, the most important type of carbon is filamentous carbon. The surface reactions, such as the methane cracking or the Boudouard reaction, produce adsorbed carbon atoms. The surface carbon atoms would dissolve into the nickel particle at the gas side, and diffuse to the rear, at the support side. At top of the nickel particle, a selvedge with high concentration is created because of the carbon isolation in nickel: The surface is enriched with carbon, and the carbon concentration decreases from the surface concentration to the bulk concentration of interstitially dissolved carbon over a number of atomic layers.

The driving force for the bulk diffusion of carbon through the metal particle is described either to a temperature gradient (Baker et al., 1972; Yang et al., 1989) or to a concentration gradient (Rostrup-Nielsen et al., 1977; Kock et al., 1985; Alstrup et

al.,1988). At the coking threshold, the gas phase carbon solubility equals to the solubility of filamentous carbon in nickel. The filamentous carbon will be formed by the formation of a solution of carbon in nickel that is saturated with respect to filamentous carbon. The degree of saturation is determined by the affinity for carbon formation of the gas phase. It was experimentally observed that the formation of filamentous carbon is much more difficult under conditions with a low affinity for carbon formation. Low temperature and low gas phase concentration of methane lead to a slow nucleation, very long periods of increasing rate of carbon formation, and also a small number of carbon filaments that is able to nucleate under these conditions.

### 2.1.4 Catalyst Development for carbon dioxide reforming of methane

#### *Active Components*

The role of suitable catalysts would not be only to speed up the overall reaction but also to adjust the appropriate elementary steps in a way which prevents both net carbon deposition and water formation. During long time ago, many experiments were performed to investigate suitable catalyst for preventing carbon deposition and water formation (both of which are thermodynamically possible).

Group VIII elements in their reduced forms, especially, Ni, Ru, Rh, Pd, Ir and Pt, are effective catalytic components, except OS, which has no activity data. Fe appears to be the only inactive Group VIII element. Because of the presence in these catalysts of a support, the difference of support-active metal interactions cause an uncertain factor in the determination of the activity of the catalytic component. In summary, supported Rh catalysts appear to be the most suitable. Ni catalysts deserve closer attention due to their high performance and lower material costs. Many investigations studied supported nickel catalyst in term of catalyst developing and identifying reaction conditions for coke-free operation. Other Group VIII elements (Co, Ru, Pd, Ir or Pt) could also be effective when put on suitable supports.

*Catalyst supports*

Since the degree of dispersion of active elements over the support and the specific metal-support interactions are different for different supports, variations in activity are expected as a result of the use of different support materials. For nickel catalysts, $Al_2O_3$, $MgO$, $Eu_2O_3$, $SiO_2$, $TiO_2$ or mixed oxides, such as., $SiO_2$-$Al_2O_3$, $MgO$- $Al_2O_3$, $CaO$- $Al_2O_3$, etc., have been used as catalyst supports with good results. However, with using the same kind of catalyst support and active component, the difference in catalyst preparation methods would result in different surface morphology of the obtained catalysts. Changing catalyst preparation method can cause different sintering resistant, e.g., from calcinations. It should be noted that for the evaluation of catalyst stability it is essential to consider the effect of sintering under reaction conditions.

Low loadings of the second and third row metals, such as Ru or Ir, are usually sufficient for very effective supported catalyst (Perera et al., 1991). However, Ni and Co catalysts required higher loadings of metals since the metal-support interactions are stronger than the case with the heavier metals. Strong metal-support interactions require that the catalysts be reduced at temperatures much higher than that required for the reduction from an oxide.

## 2.2 Periodic operation

The terms periodic operation, cycling or cyclic operation, modulation and forcing or periodic forcing, can be used interchangeably. They refer to an operation in which one or more inputs into a chemical reactor vary with time, but in such a way that each input is revisited after a time corresponding to the period. Figure 2.2 shows a typical example of the periodic operation of a reactor. Two inputs, the volumetric flow rates of reactants 'A' and 'B', are switched periodically between two values and generate a chain of step-changes representing a square-wave variation of reactant concentrations in the reactor feed. In most of the systems studied in the laboratory, the flow rate variations are matched so that the space velocity in the reactor remains constant, but this is not a necessary condition. The figure typifies the system most

frequently studied. However, other inputs may be varied, such as reactor temperature, flow rate, and flow direction.

Comparison between periodic operation and steady-state operation is shown in Figure 2.3. Input variations result in a time-varying output shown in the upper right of the figure. These are referred to as instantaneous concentrations, yields, or rates. The more important information is the mean or time-average production rate, and yield or product concentration.

There are some variables to be introduced for understanding about periodic operation (see Figure 2.3);

Period ($\tau$)      --   The time between repetitions of a change in an input condition;

Split (s)       --   The duration of one part of cycle relative to the period;

Amplitude (A) --   The change in the value of an input condition between its
                    highest and mean values.

The split, sometimes referred to as the duty fraction, measures the symmetry of a cycle. At the value, s = 0.5 indicates a symmetrical cycle with both parts of equal duration. Split must be defined relative to one of the reactants. The split measures the relative duration of the portion of the cycle in which that reactant is at its highest concentration. Amplitude takes on just a single value for symmetrical forcing, but, if s $\neq$ 0.5, and need to keep the space velocity in the reactor remains constant, two amplitude values must be given, one for each portion of the cycle.

Another variable is the phase lag. The composition changes shown in Figure 2.3 are 180 ° or ¶ radians out-of-phase. Other phase lags could be used. Such as in a pulsing operation, the phase lag is zero. In principle, temperature, pressure, or even flow velocity could be varied. The choice of inputs, mode of variation, and cycle structure are depend on the strategy.

The advantages of periodic operation could be summarized as follows:
- Increased catalyst activity, expressed as conversion or rate of reaction, especially for reactions in which conversion per pass is limited, often by

equilibrium. For example, Rambeau et al. (1981) found that yield of acrolein in the partial oxidation of propene over Sb-SnO catalyst, can be doubled by switching between air and propene mixtures of different composition.

- Periodic operation may be a means of permitting reactors to operate safely in regions of high parametric sensitivity, such as, in exothermic reaction, for example, Jain et al. (1982), who worked with ammonia synthesis, demonstrated that composition forcing smooth the reactor temperature distribution and reduces peak temperatures, while maintaining the conversion achieved under steady state.

- Controlling of catalyst deactivation could be attainable by forced modulation. There is evident that periodic operation can decrease the rate of catalyst deactivation, for example, Chanchlani et al. (1992) performed methanol synthesis deactivation experiment using a $Cu/ZnO/Al_2O_3$ catalyst, and found that the loss of activity is clearly less for composition forcing between $H_2$ and CO than steady state reaction.

For strategy in periodic operations, there are many ways for operating a reactor periodically. At least two components are required for composition modulation. These could be two reactants or a reactant and a non-reactant (either a promoter or an inert). This limiting case, shown as two reactant cycles in Figure 2.4, presents two strategy options from a study of methanol synthesis. Moreover, there is an alternative to operate by varying any periodical variables, such as, period and split of each cycle for investigation the optimizing of scoped reaction.

Although only two-part cycles are shown in Figure. 2.4, multi-part cycles are possible. Multi-part cycles could be useful in some circumstances, such as flushing the catalyst surface by inert gas to desorbed reactant or product before exposing the surface to a second reactant, as be showed in Figure 2.5
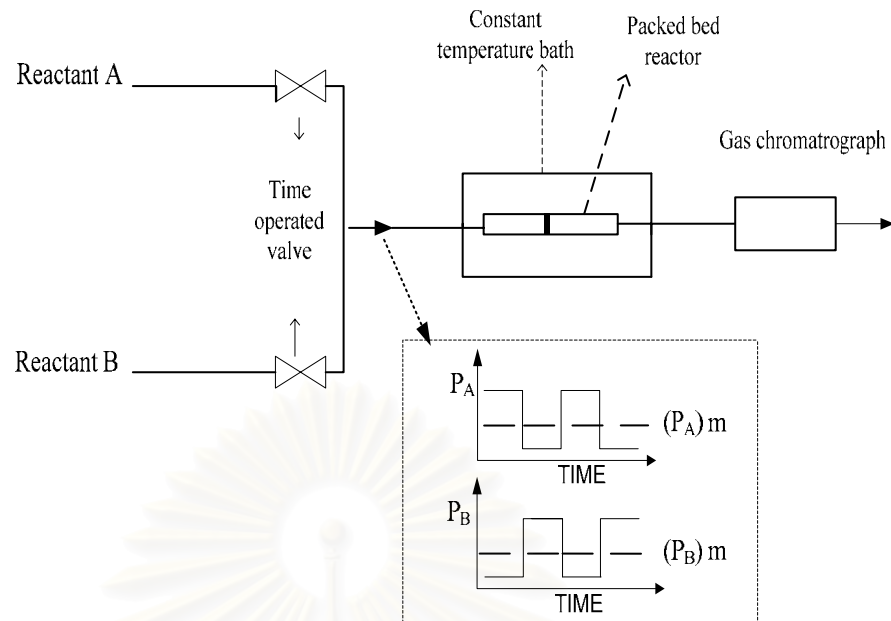
**Figure 2.2** Schematic diagram of periodically operating reactor for two feed streams
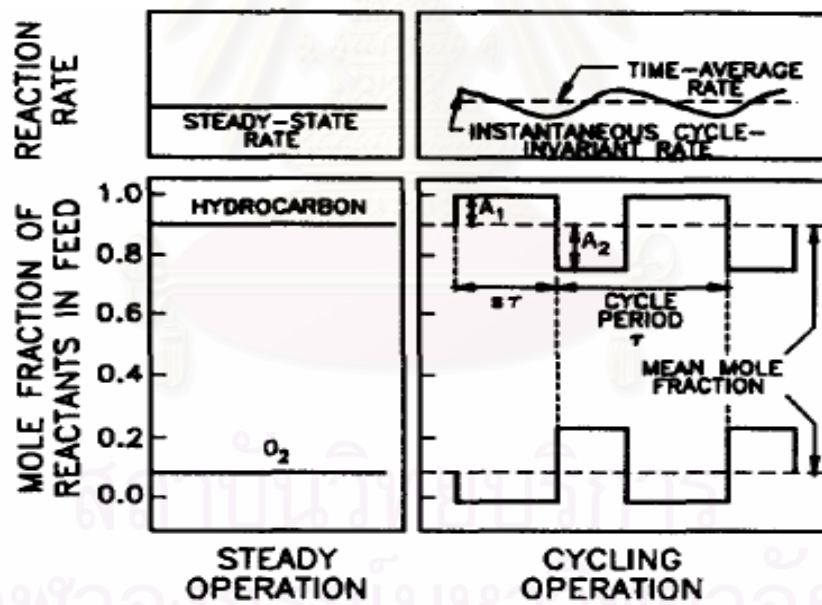


**Figure 2.3** Comparison of steady state (left side) and periodic (right side) operation showing definition of the cycling variables: cycle period (frequency), r, cycle split (duty fraction), s; amplitudes, $A_1, A_2$. (Silveston, 1995)
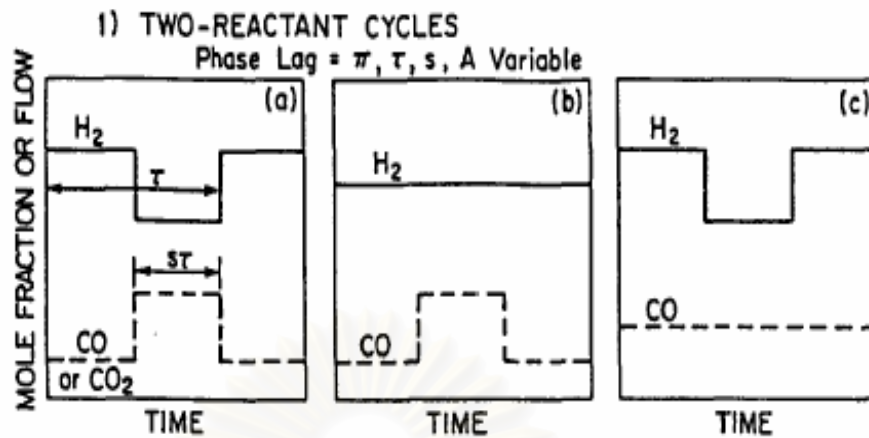
**Figure 2.4** Different possible composition forcing operations with two components (reactants and/ or diluents) for methanol synthesis (Chanchlani, 1994).
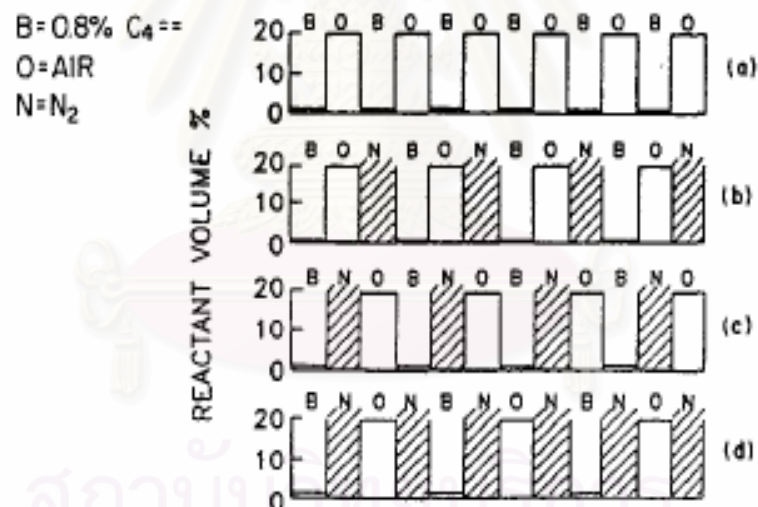


**Figure 2.5** Modulation strategies with two-, three-, and four-part cycles for partial oxidation of butadiene to Maleic Anhydride with and without diluent flushing (Lang, 1991).

# CHAPTER III
# LITERATURE REVIEW

The reforming of methane with carbon dioxide produces synthesis gas with a lower $H_2/CO$ ratio than that generated by the widely employed steam reforming reaction. This process is also a particularly efficient process for producing synthesis gas from both green house gasses, methane and carbon dioxide. Unfortunately, the disadvantage of dry reforming process is a greater potential for carbon formation, primarily due to the lower H/C ratio of this system. Many researches have been carried out on the development of effective catalysts and carbon-free conditions for this reaction but only a few studies have focused on the new alternative of the contacting technique under transient condition with periodic operation.

The literature review is divided into two main parts, i.e., (a) Research and development on methane reforming with carbon dioxide, (b) Recent studies of catalytic cracking of methane and catalyst regeneration. An attempt will also be made to summarise the present knowledge and understanding of various factors influencing the performance of the carbon dioxide reforming of methane. In the last section of this review, comments on previous studies that have directly influenced the aims of this study are given.

## 3.1 Literature reviews

### 3.1.1 Effect of types of catalyst and support for carbon dioxide reforming of methane

The carbon dioxide reforming of methane was first studied by Fischer and Tropsch (1928) over a number of base metal catalysts. Calculations indicate that the reaction is thermodynamically favored above 913 K. It is more endothermic than steam reforming reaction. Carbon deposition was predicted and carbon formation over metal catalysts during the carbon dioxide reforming reaction has been observed (Gadalla *et al.*, 1988). An industrial process, the Calcor process, has been developed, which uses methane and a large excess of carbon dioxide to make carbon monoxide

rich synthesis gas, a nickel based catalyst was employed (Teuner *et al*., 1985; Kurz *et al*., 1990).

Nobel metals such as Pt, Pd, and especially Rh, are fairly stable for the reaction. Richardson *et al.*(1990) and Basini *et al.*(1991) revealed that Rh is a better material after considering the overall performance criteria, e.g., high activity, high $H_2$ selectivity and carbon-free operation. Rh catalysts give near equilibrium conversions over a wide range of space velocity, by the small difference between the carbon dioxide and methane conversion. However, they are too expensive to utilize Rh practically. Inexpensive base metals such as Fe, Co and Ni are also known to be active for the reaction to some extent, and among them, Ni is the most promising. The main drawback of a conventional Ni-based catalyst is its poor stability, mainly caused by a high-coking rate. Carbonaceous deposition can result in pressure drop and plugging problem in the reactor. Consequently, many researches have been currently carried out to improve both performance and lifetime of Ni-based catalyst.

From early research on the effect of catalyst support, Uchijima *et al.* (1993), working with $Rh/SiO_2$, observed promotional effects for both the carbon dioxide reforming of methane and RWGS reactions when some $Al_2O_3$, $TiO_2$ or MgO was added to the catalyst. Moreover, Takano *et al* (1994, 1996) investigated the reforming of methane with carbon dioxide using various Ni catalysts, including industrial stream reforming catalyst and industrial methanation catalyst. Among various supports, catalyst activity varied with the kind of support according to the following order; $Al_2O_3 > SiO_2$ with $MgO > SiO_2$ It was therefore argued that the promotional effect for carbon dioxide reforming could not be due to difference in metal distribution or the metal-support interaction.

It was interpreted in terms of carbon dioxide activation and the role of the mildly basic oxide in sufficiently improving the adsorption strength of carbon dioxide (in the form of carbonate or formate) for it to migrate to the active Rh an Ni sites. $Al_2O_3$ has basic nature, not like $SiO_2$. Addition of $SiO_2$ with MgO would increase the basicity of the support than only $SiO_2$ because of their base nature. This interpretation is in line with the mechanism suggested for carbon dioxide activation on alkali metal-containing platinum group metals (Solymosi *et al.*, 1991), it is also documented that

some oxide supports exert significant influence on the reactivity of carbon that forms on the surface of the catalytic metals (Solymosi *et al.*, 1993).

Several Ni catalysts with long life and high activities have been reported in many literatures. These include $Ni/Al_2O_3$ (Takano *et al.*, 1994,1996; Ito *et al.*, 1999), $Ni/TiO_2$ (Masai *et al.*, 1988), $Ni/CeO_2$ (Asmi *et al.*, 2003), Ni/Perovskite (Goldwasser *et al.*, 2003), and $Ni/Ce-ZrO_2$ (Lee *et al.*, 2003) modified catalyst. It is noted that these catalysts contain basic support or additive. It has been suggested that carbon decomposition can be suppressed when nickel is deposited on the supports possessing strong Lewis basicity, which can be achieved, by addition of alkaline earth oxides to the support. Because carbon dioxide is well known as an acid gas, the increase in the Lewis basicity is expected to strengthen the ability of the catalyst to chemisorb carbon dioxide and, to reduce carbon formation via Boudouard reaction by shifting the equilibrium concentration. On the other hand, the addition of basic promoters can also lead to both catalyst stability and the enhancement of deposited carbon.

Moreover, using Ni catalyst on the other kinds of support, such as on the ceramic foam, which was a macro porous medium, was also investigated. According to the research of *Takano et al.* (1994,1996), the ceramics foam codiarite coat $Al_2O_3$ supports catalyst show high activity with a good stability and suppressed the increase of pressure drop in continuous flow reactor due to its high porosity.

The effect of Ni diameter was also investigated. It was indicated that the amount of carbonaceous deposits based on the surface Ni atom increased as the diameter of Ni increased. So that, it was presumed that catalyst with larger Ni diameter enhanced plugging more readily.

Furthermore, addition of a promoter to Ni catalyst has been used to lower the rate of coke deposition. Doping of some kind of metals such as Sn (Hou *et al.*, 2004) or Ca (Hou *et al.*, 2003) in a small amount in $Ni/Al_2O_3$ catalyst improved the dispersion and increased the reducibility of Ni catalyst and retarded the sintering of active Ni particle, which could improve the stability of the catalyst. Because the coke formation would require a bigger ensemble sites, the formation of surface intermetallic compound (such as $Ni_3Sn$), hindered the dissolution of carbon in Ni

crystals. While adding Potassium metal in NiK/Al$_2$O$_3$ (Juan-Juan *et al*., 2004) promoted the reduction of Ni and hindered the coke deposition. This species gasified coke without any structural modification of nickel during reaction at 973 K. However, the surface enriched with these additives in excess amount, would hinder the access of CH$_4$ and/or CO$_2$ on the surface of Ni particles and depress its activity.

**3.1.2 Effects of operating parameters on carbon dioxide reforming of methane**

Many researches have been investigated to study the effects of many operating parameters on carbon dioxide reforming of methane over several kind of supported catalysts, with experimental variables of temperature, CO$_2$/CH$_4$ feed ratio, and pressure.

- **Effect of reaction temperature**

Takano *et al*., (1994, 1996) reported that conversion of methane increases with increasing of reaction temperature. For Ni/SiO$_2$,MgO catalyst, the pressure drop in reactor increased at temperature below 1000 K, did not change during the reaction temperature of 1030 K and decreased at higher temperature than 1060 K. This suggested that the rate of deposition and decomposition of carbonaceous deposits balanced at 1030 K.

The conclusion above is in line with Fraenkel *et al*., (1986), who investigated the reforming reaction at the temperature range from 400-1000°C using a CO$_2$/CH$_4$ feed ratio of l/l at pressures of 1 and 10 atmospheres. They indicated that conversion of methane would be lift up with higher reaction temperature. At 900°C the methane conversions are 97 and 90% at 1 and 10 atmospheres, respectively. The report also indicated that formation of water decreased with increasing temperature. The formation of water effectively disappears above about 900°C, due to less thermodynamically feasible at high reaction temperature.

- **Effect of feed ratio of CO$_2$/ CH$_4$**

The investigations were conducted by varying ratio of reactants CO$_2$/CH$_4$ from 0.5 to 5 over Ni/Al$_2$O$_3$ catalyst (Takano *et al*., 1994, 1996) and from 0 to 1.6 over

Pt/Al$_2$O$_3$ catalyst (Gustafson *et al.*, 1991). Conversion of methane increases with the increase of feed ratio of CO$_2$/CH$_4$. A lower CO$_2$/CH$_4$ ratio was preferred in order to increase the selectivity to H$_2$. The product CO/H$_2$ ratio proceeds towards unity as carbon dioxide in the feed is reduced, indicating that the hydrogen consumption resulted from RWGS reaction is increasingly restricted due to the unavailability of carbon dioxide. Nevertheless, increasing CO$_2$/CH$_4$ ratio would decrease carbonaceous deposition and pressure drop in the plug flow reactor.

- **Effect of pressure of system**

The partial pressure of carbon dioxide has no influence on reaction rate, but the apparent reaction order with respect to CH$_4$ partial pressure was found to be between 0.8 and 1, depending on type of supported catalyst. Therefore, the reaction rate can be expressed approximately through the simple law equation (Takano *et al.*, 1994, 1996).

$$- r_{CH_4} = k\left(P_{CH_4}\right)^m \qquad \text{(m=0.8-1)}$$

Concerning the effect of operating pressure, Fraenkel *et al.*(1986) derived the thermodynamic equilibrium under two different pressures of 1 and 10 atmospheres. The carbon deposition threshold curves indicated that carbon deposition is thermodynamically possible for a CO$_2$/CH$_4$ reforming feed ratio of l/l at temperatures up to 1000°C at 1 atmosphere and 1100°C at 10 atmospheres. Moreover, at the same reaction condition, conversion of CH$_4$ would be reduced with increasing total pressure.

**3.1.3 Effect of other feed reactant on carbon dioxide reforming of methane**

The addition of another reactant, especially oxygen could combine exothermic partial oxidation with carbon dioxide reforming of methane, which can utilize energy from partial oxidation and allow the production of syngas with a wider range of H$_2$/CO ratios between 1 to 2 (Souza *et al.*, 2003; Jing *et al.*, 2004). The result showed that addition of oxygen to the feed increases methane conversion and decreases the

hydrogen selectivity. The loss of catalyst activity with time on stream decreased with increasing the amount of oxygen added. Moreover, combining reaction improves the temperature control and reduces the formation of hot spot from only partial oxidation. The addition of $O_2$ also reduces carbonaceous deposition by oxidation with coke, maintaining the stability of catalyst. However, the performance of these reactions depends on the ratio of $O_2$: $CH_4$: $CO_2$ and the kind of catalysts.

### 3.1.4 Catalytic cracking of methane and catalyst regeneration reaction

The direct cracking of methane over supported nickel catalysts has recently been receiving attention as an alternative route for production of hydrogen from natural gas ($CH_4 = C + 2H_2$). Unlike other processes, which produce a mixture of hydrogen, water, and carbon oxides, catalytic cracking produces hydrogen and solid carbon, eliminating the necessity for the separation of hydrogen from the other gaseous products.

The direct cracking of methane was early investigated by Claridge *et al.* (1993). They investigated the rates of carbon deposition for the system with pure methane and pure carbon monoxide over a supported nickel catalyst at various temperatures. The Boudouard and methane decomposition reactions are both thermodynamically favorable. They showed that both reactions are catalyzed but with varying extents depending on the operating temperature. At about 1050 K, the amount of carbon from pure carbon monoxide via the Boudouard reaction was very low compared with the amount from the methane decomposition reaction (20 times).

In order to enhance carbon production from $CH_4$ cracking, Ermakova *et al.* (2002) used Ni/$SiO_2$ catalysts prepared by heterophase sol-gel method with various stages of catalyst preparation. The carbon yield is demonstrated to depend only on the interaction between nickel and silica. The presence of silicates about 2 wt% in the 90% Ni–10% $SiO_2$ catalyst shows a rapid catalyst deactivation (the carbon yield is 40 g C/g Ni). The carbon yield as high as 384 g C/g Ni is observed with silicate-free 90% Ni–10% $SiO_2$ catalyst. It is assumed that silicate can either inhibit or promote formation of carbon depending on their amount comprised in Ni/ $SiO_2$ catalysts.

Zhang *et al*. (1998) performed the catalytic cracking of methane over silica-supported Ni catalyst at 823 K. These catalysts maintained their activity for a sustained period of time because of their capability to accumulate large amounts of carbon on their surface in the form of long cylindrical hollow filaments, with a nickel particle located at the front tip of each individual filament. Deactivation of catalyst occurs due to spatial limitations imposed on the filament growth, which lead to the loss of exposed surface.

In addition, they also studied regeneration of catalysts by oxidation in air ($C + O_2 = CO_2$) and steam gasification ($C + xH_2O = xH_2 + CO_x$) of deposited carbon. Both methods appear to be able to fully restore the activity of the catalyst. The oxidation process was faster than the steam gasification, but can cause a high temperature front, which causes the collapse of catalyst bed to the fine powder due to this highly exothermic reaction. The XRD pattern suggests that the oxidation process completely removes the deposited carbon and converts the metallic nickel into nickel oxide, which needs to be reduced before next reaction cycle.

On the contrary, the catalyst bed maintained the uniform temperature profile during the steam regeneration process and catalyst preserved its metallic metal nickel form at the end of process. Furthermore, the steam gasification leads to the production of the additional hydrogen with carbon monoxide and methane as secondary products, formed due to the reverse water-gas shift ($CO_2 + H_2 = CO + H_2O$) and methanation ($CO + 3H_2 = CH_4 + H_2O$) reactions.

Later, Aiello *et al*. (2000) investigated the catalytic cracking of methane followed by steam regeneration over 15 wt% $Ni/SiO_2$ catalyst with several repeated cracking/regeneration cycles. The results showed that a 15 wt% $Ni/SiO_2$ catalyst can be fully regenerated at 923 K with steam for up to 10 successive cracking/regeneration cycles without any significant loss of catalytic activity. XRD analyses indicate no increase in the amount of carbon remaining on the spent catalyst and no structural changes in the nickel regenerated particles.

Moreover, there also had a research on catalytic cracking of methane followed by catalyst regeneration with oxygen. Monnerat *et al*. (2001) performed the

experiment by operating reactor periodically with the cracking reaction followed by the catalyst regeneration by burning of coke on Ni-gauze catalyst in oxidative oxygen atmosphere. They reported that efficient hydrogen production occurs at temperatures of 773 K while the influence of cycle time on the time-average hydrogen performance (molar flow rate of $H_2$/cycle period duration, mmol/min) shows a maximum for a cycle time of 4 min while the selectivity of carbon oxides are not influenced by the cycle duration. The influence of the cycle split on the time-average hydrogen performance shows that a maximum value is attained $\gamma = 0.5$.

Another method for suppression of carbonaceous deposition is "D-R treatment". This pretreatment of catalyst was conducted on $Ni/Al_2O_3$ catalyst according to the paper of Ito *et al*. (1999), which is based on the hypothesis that active cores forming carbon whiskers are different from surface active sites for the main reaction on the catalyst. For this technique, one cycle consists of two steps. In the deposition (D) step, methane was introduced to cause carbonaceous deposition and to grow carbon whiskers at 1000 K for 1 hour. The catalyst, which only participates in carbonaceous is detached from support. In the removal (R) step, carbon dioxde was introduced to remove carbon whiskers ($CO_2 + C = 2CO$) at 1000 K for 1 hour. In this step, the growing cores with catalyst are removed and deactivated. The cycle is repeated several times.

The D-R treatment decreased the bulk nickel because a part of the nickel was removed from catalyst, which became the growing cores of carbon whiskers, and made catalyst inactive for carbonaceous deposition. This treatment accelerated the reforming activity, because the nickel located near the support was not influenced by the D-R treatment and the new sites for the reforming reaction were exposed by the removal of the bulk catalyst.

## 3.2 Comment on previous works

From the previous studies, there are many researchers considering the carbon dioxide reforming of methane. Most of related investigations concerned about catalyst development in terms of catalytic activity and durability of catalyst, while investigations about suitable condition for operation is not widely studied. Although

many reactions have been reported to show better performance when operated under periodic mode, the previous studies have not implemented this operation to this reaction.

From literature survey on catalytic cracking of methane, $O_2$ and steam ($H_2O$) are generally introduced to regenerate spent catalysts from cracking period. Moreover, most studies extend regeneration period to ensure that deposited coke have to be removed completely. There is no research focusing on suitable duration time for the system using carbon dioxide as an oxidizing agent in regeneration period. Therefore, periodic operation between direct catalytic cracking of methane into hydrogen and carbon, and catalyst regeneration in oxidative atmosphere of carbon dioxide to produce carbon monoxide is chosen for study in this research.

# CHAPTER IV
# EXPERIMENTS

This chapter describes experimental systems and procedures used in this study. The catalyst, dilution material, and reactant gases for the experiment are summarized in Section 4.1. The details of apparatus for studying the reforming reaction are provided in Section 4.2. Finally, the reaction procedures are illustrated in Section 4.3.

## 4.1 Chemicals

### 4.1.1 Catalyst

An industrial steam reforming catalyst, $Ni/SiO_2.MgO$, was employed for the carbon dioxide reforming of methane in this research. More details of catalyst characteristics are shown in Table 4.1

**Table 4.1** The specific properties of catalyst used in this study

| Catalyst | N 185 |
|---|---|
| Ni content | 55 wt% |
| Support/co-catalyst | $SiO_2$, MgO |
| Surface area [$m^2$/kg] | $1.23 \times 10^5$ |
| Ni Surface area [$m^2$/kg] | $8.37 \times 10^3$ |
| Ni Diameter [nm] | 44 |

### 4.1.2 Dilution material

A dilution material was uniformly mixed and packed with the catalyst in the reactor to reduce the bed pressure drop due to carbon formation from the reaction and to reduce temperature gradients along the catalyst bed. Silicon carbide (SiC) was chosen as

a dilution material due to its excellent stability at high temperature. The average size of silicon carbide was 200-450 mesh. In all studies, 0.3 g of catalyst was mixed with 1 g of silicon carbide.

### 4.1.3 Reactant gases

The reactant gases used for the reaction study were ultra high purity (99.999 %) of carbon dioxide and ultra high purity (99.999%) of methane supplied by Thai Industrial Gas Limited (TIG). Ultra high purity $H_2$ was used for reducing catalyst from NiO form to Ni metallic form before each experiment while ultra high purity argon was used for purging the apparatus system.

## 4.2 Apparatus

Flow diagram of a lab-scale gas phase carbon dioxide reforming of methane system is shown in Figure 4.1. The system consists of a reactor, an automatic temperature controller, an electrical furnace and a gas controlling system.

### 4.2.1 Reactor

The reaction was performed in a conventional quartz tube (inside diameter = 11 mm) at atmospheric pressure. Two sampling points were located before and after the catalyst bed. Catalyst was placed over a quartz wool layer for supporting the weight of catalyst bed and coke which could be formed during the reaction.

### 4.2.2 Automatic Temperature Controller

This unit consisted of a magnetic solid state relay switch connected to a variable voltage transformer and a temperature controller connected to a thermocouple. Reactor temperature was measured by thermocouple which was placed in the furnace at the

position of the catalyst bed. The temperature control set point is adjustable within the range of 0-1,000$^{\circ}$C at the maximum voltage output of 220 V.

### 4.2.3 Electrical Furnace

The furnace with 2 kW heating coil was connected with the automatic temperature controller to supply heat to the reactor. The reactor could be operated from room temperature up to 800$^{\circ}$C at the maximum voltage of 220 V.

### 4.2.4 Gas Controlling System

Each reactant gas was equipped with a pressure gas regulator (0-120 psig) and an on-off valve. A flow rate was controlled by adjusting a needle valve. For periodic operation, each reactant feed was switched between opening and closing periodically by using a solenoid valve (Flon industry, Japan) controlled by a multi timer (Sibata BT-3).

### 4.2.5 Gas Chromatography

A gas chromatography Shimadzu modal 8A (GC-8A) equipped with a thermal conductivity detector (TCD) was used to analyze gas composition. Methane in feed stream, carbon monoxide and hydrogen in the product streams were analyzed using Molecular sieve 5A column. Carbon dioxide in the product stream was analyzed by using Poropak-Q column. The operating conditions for the gas chromatography are shown in Table 4.2.

**Table 4.2** Operating conditions for gas chromatograph

| Gas Chromatograph | Shimadzu GC-8A | |
|---|---|---|
| Detector | TCD | |
| Column | Molecular sieve 5A | Porapak-Q |
| - Column material | SUS | SUS |
| - Length (m) | 2 | - |
| - Outer diameter (mm) | 4 | - |
| - Inner diameter (mm) | 3 | - |
| - Mesh range | 60/80 | - |
| - Maximum temperature ($^o$C) | 350 | - |
| Carrier gas | Ar (99.999%) | Ar (99.999%) |
| Carrier gas flow (ml/min) | 30 | 30 |
| Column temperature - initial ($^o$C) - final ($^o$C) | 70 70 | 70 70 |
| Injector temperature ($^o$C) | 100 | 100 |
| Detector temperature ($^o$C) | 100 | 100 |
| Current (mA) | 70 | 70 |
| Analyzed gas | $CH_4$, $H_2$, CO | $CO_2$ |

### 4.2.6  X-ray diffraction (XRD)

The crystallinity and X-ray diffraction patterns of the fresh and spent catalysts were performed by an X-ray diffractometer, SIEMENS D5000, using Cu Kα radiation with Ni filter.  The operating conditions of measurement  are shown below :

2θ range of detection :          10-80$^o$

Resolution :                0.04$^o$

Number of scan              20

### 4.2.7 Scanning electron microscopy (SEM)

Scanning electron microscopy (SEM) was used to determine the catalyst granule morphology, using a JEOL JSM-35CF scanning electron microscope.  The SEM was operated using the back scattering electron (BSE) mode at 15 kV at Scientific and Technological Reseach Equipment Centre, Chulalongkorn University (STREC).

## 4.3 Experimental procedures

The experimental procedures are described in details below.

1)  The mixture of 55 wt% $Ni/SiO_2,MgO$ (0.3 g) and silicon carbide (1 g) was packed in the middle of quartz tubular reactor located in the electrical furnace. Flow rates of methane and carbon dioxide were adjusted to desired values. For a steady state operation experiment the flow rate of each gas was set at 12.5 cc/min. For a periodic operation experiment, flow rate of each reactant varied with operating condition (cycle time and cycle split); however, its time-average flow rate is kept at the same value of the steady state operation (12.5 cc/min) for performance comparison purpose. The feed gas composition was analyzed by using the TCD gas chromatography. The chromatogram data were changed into mole of methane and carbon dioxide using a calibration curves (Appendix A).  Then the reactant feed gases were switched off using the on-off values.

2)  Argon (30 cc/min) was fed to the reactor for purging reactant gases. Then the reactor was heated up to 923 K at a rate of 5 K/min. At this temperature the argon gas was switched off and the catalyst was reduced under hydrogen flow (30 cc/min) for 1 h. After the catalyst reduction, the system was purged with argon for 10 min to remove hydrogen gas from the system and the reactor temperature was changed to a desired value.

3)  The reaction was started by feeding the reactant(s) to the catalyst bed. For the steady state operation both methane and carbon dioxide were fed simultaneously. For the

periodic operation, the multi timer was set to control the solenoid valves to allow methane to pass through the reactor for required period of time first, and then carbon dioxide for the required period of time. The operation occurred repeatedly until the end of experimental study.

4) An exit gas was sampled to analyze its composition. In case of periodic operation, product gas after completing each cracking/regeneration cycle was collected by using a sampling bag. A three-way valve was used to switch total product gas flow into another sample bag for collecting from next cracking/regeneration cycle period. A gas sample from the sampling bag was analyzed to find time-average composition of the product gas. Both sampling bag would be switched every 20 min, until the end of reaction. The reaction product was analyzed by the TCD gas chromatograph.
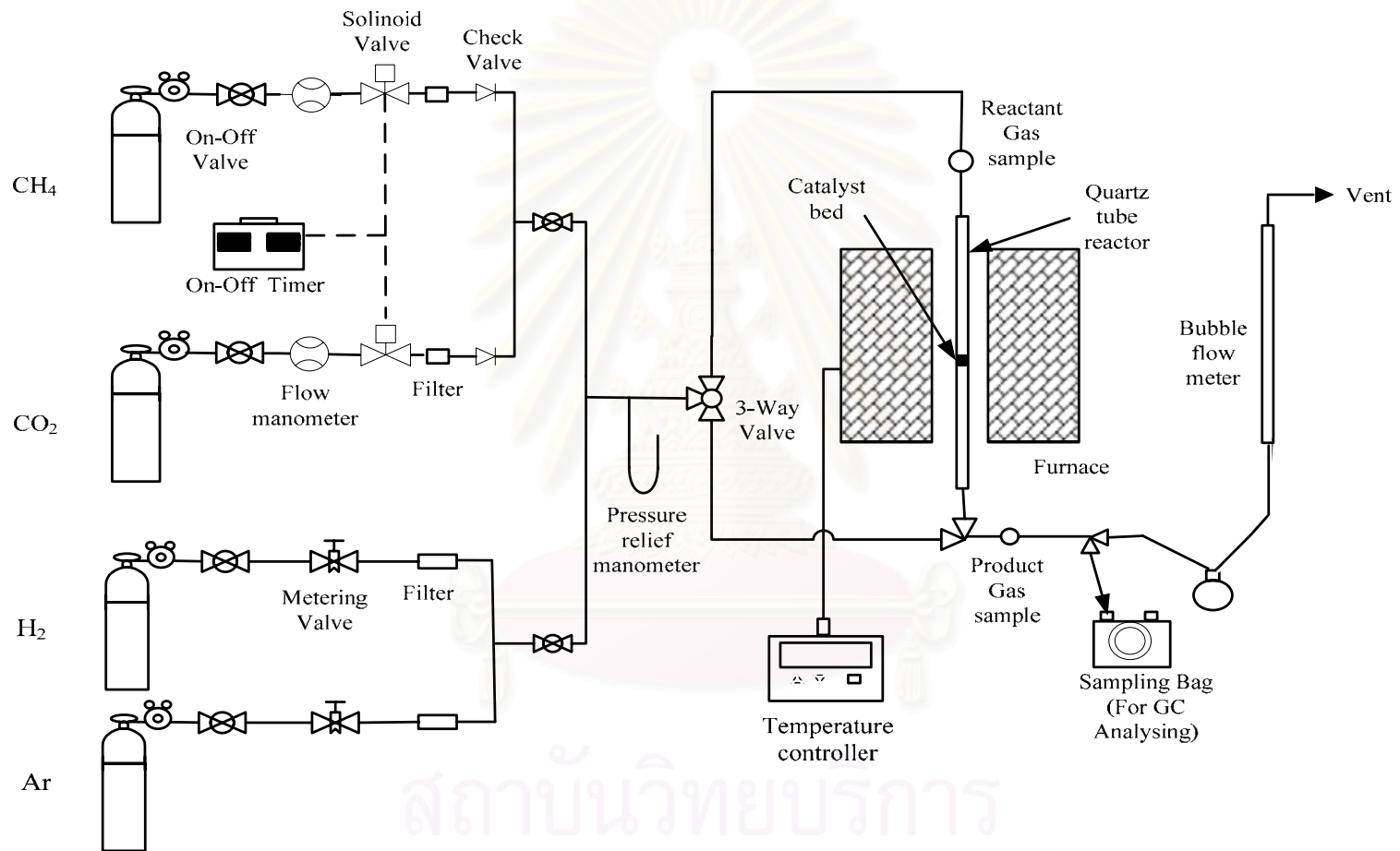
**Figure 4.1** Schematic diagram of a lab-scale gas phase for carbon dioxide reforming of methane under periodic operation

# CHAPTER V
# RESULTS AND DISCUSSION

The results and discussion in this chapter are divided into two sections. In the first section, the general characteristics of carbon dioxide reforming of methane under periodic operation were investigated. Next, their performances under different cycle periods were compared with those from the steady state operation. Moreover, the effects of other operating variables such as operating temperature and cycle split are discussed.

## 5.1 Characteristics of carbon dioxide reforming of methane under periodic operation

In this part, the behavior of the carbon dioxide reforming of methane under periodic operation was investigated. The operation consists of two main steps: (i) methane cracking and (ii) regeneration of catalyst via reverse Boudouard reaction. $Ni/SiO_2.MgO$, a commercial catalyst, was employed in all experiments in this study. At the beginning, the catalytic cracking of methane ($CH_4 \rightarrow C + H_2$) was carried out at 1023 K for determining catalyst activity along time on stream. Hydrogen and methane were the only components detected in the product stream within the TCD limits.

The methane conversion is shown in Figure 5.1. $Ni/SiO_2.MgO$ showed high conversion of methane about 73% at the start and declined rapidly to about 50% within 25 minutes. Then the conversion decreased to about 15% after 50 minutes of reaction and fell down slightly until the end of the methane feed at 225 minutes. The U-tube pressure manometer indicated stable pressure drop in the first period of reaction. After 20 minutes, the pressure drop increased gradually until reaching the plateau in about 50 minutes of time on stream. From the results, it could be presumed that catalyst would lose their activities due to carbonaceous deposition on the catalyst, which resulted in lowering conversion and increasing pressure drop within about 20 minutes.
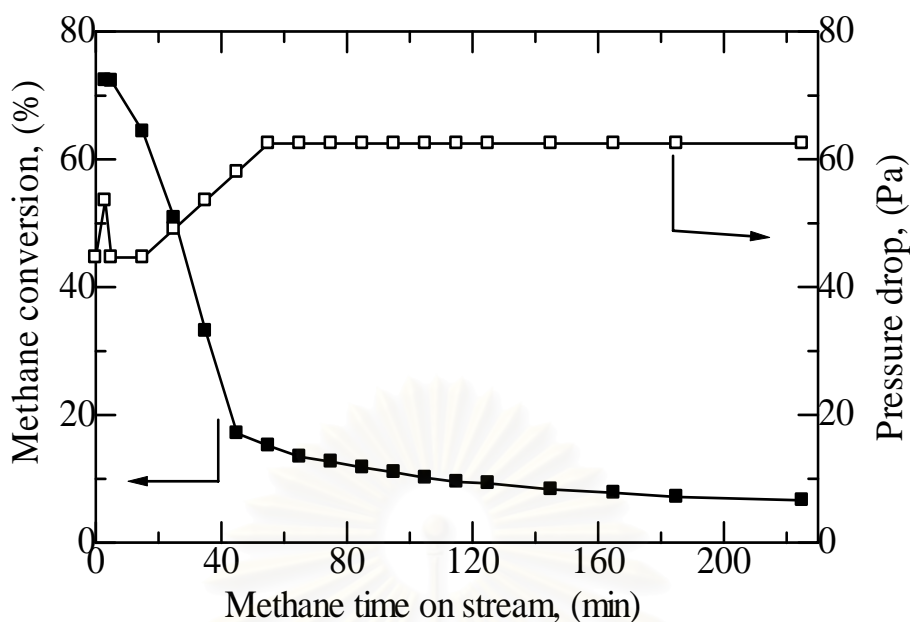
**Figure 5.1** Changes in catalytic activity (■,——); and pressure drop (□,——); of catalytic cracking of methane reaction over $Ni/SiO_2.MgO$ at 1023 K with methane flow rate of 25 ml/min and 0.3 g of catalyst.

After testing catalytic activity for the methane cracking, the catalyst regeneration with carbon dioxide at 1023 K was performed to investigate the time to restore spent catalyst. In this part, methane cracking at the same condition was conducted; however, the cracking period was limited at 25 minutes to prevent complete deactivation with coke formation. Figure 5.2 shows the pictures of the catalyst bed before and after the reaction for 25 minutes. It is obvious that significant amount of coke was accumulated from the methane cracking. The catalyst regeneration was carried out by changing the feed from methane to carbon dioxide (25 ml/min). Carbon monoxide was detected as a main product according to the reverse Boudouard reaction ($C + CO_2 \rightarrow 2CO$).

Figure 5.3 shows the carbon dioxide conversion for the spent catalyst which was exposed to the methane cracking for 25 minutes. The conversion of carbon dioxide was stable at about 54% for 20 minutes and then decreased steeply to about 3% after 30 minutes of time on stream. Pressure drop decreased gradually from 60 Pa to 30 Pa in about 25 minutes, and declined slightly until stopping the feed.
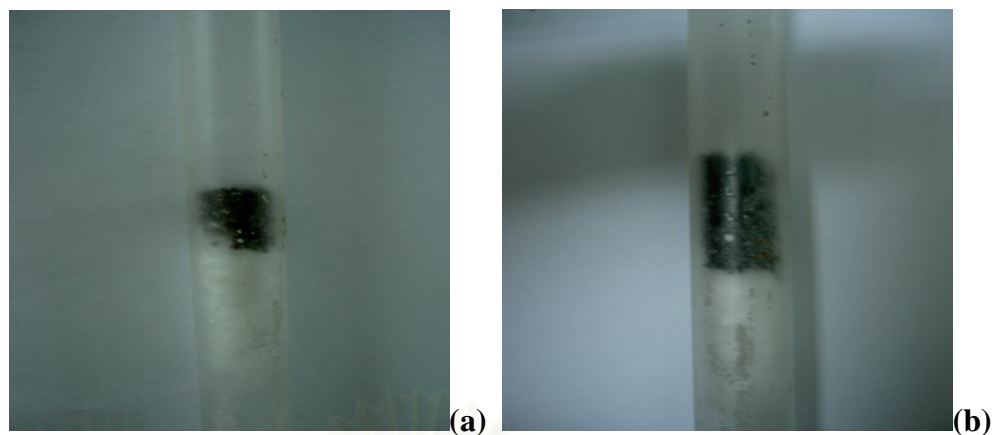
**Figure 5.2** Ni/SiO$_2$.MgO Catalyst bed: (a) Before catalytic cracking of methane reaction, (b) After cracking period at 1023 K for 25 min.

It is expected that most of deposited coke could be removed from the spent catalyst within about 20 minutes of the regeneration step by reacting with carbon dioxide. From the above results, the further studies were performed using the cracking period not to exceed 20 minutes for preventing complete deactivation of catalyst. Moreover, regeneration period with carbon dioxide was kept not over 20 minutes to allow an efficient utilization of carbon dioxide.
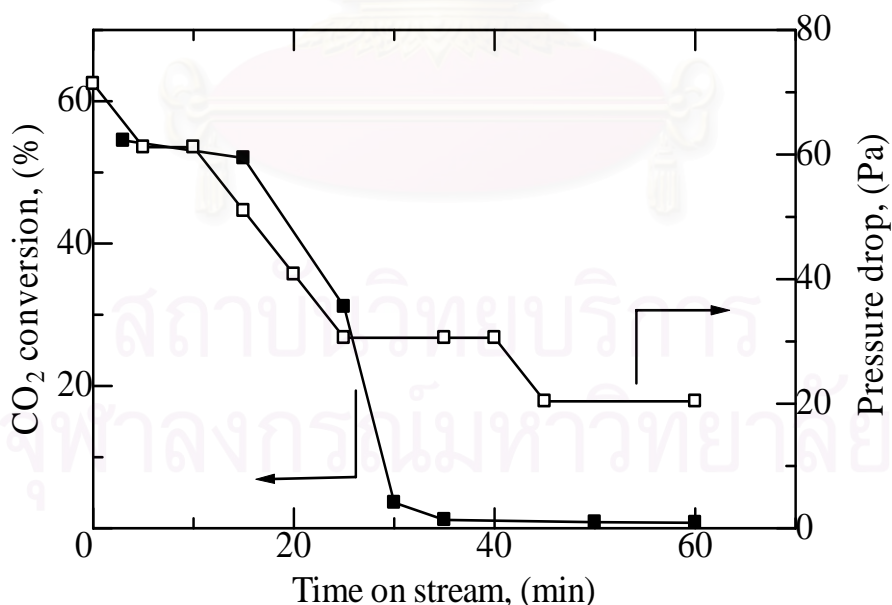


**Figure 5.3** Changes in conversion of carbon dioxide (■,——); and pressure drop (□,——); over spent Ni/SiO$_2$.MgO catalyst after 25 min of methane cracking at 1023 K with CO$_2$ flow rate of 25 ml/min and 0.3 g of catalyst.

## 5.2 Performance comparison of carbon dioxide reforming of methane under periodic operation and steady state operation

Performance comparison was considered for two cases of interest: (i) steady state operation and (ii) periodic operation. All experiments were conducted at 1023 K, atmospheric pressure and total reaction time of 200 minutes. For the steady state operation, a mixture of methane (12.5 cc/min) and carbon dioxide (12.5 cc/min) was allowed to flow through the catalyst bed in the reactor. For the periodic operation, the experiments were performed using a constant cycle split ($s$) of 0.5 and the flow rate of each reactant was kept at 25 cc/min. The cycle period was varied at 40 minutes (5 cycles), 20 minutes (10 cycles), and 10 minutes (20 cycles). It should be noted that the time-average feed flow rates were equivalent for all experiments so that the performance comparison was based on the same feed rates.

Figure 5.4 shows the profiles of methane conversion with time on stream for both steady state and periodic operations. The methane conversion of the periodic operation was time-average conversion calculated from average composition of gas product collected after the end of each cracking/regeneration cycle. It was found that the steady state operation offered a stable methane conversion at 90%, indicating no significant deactivation at least within 200 minutes of time on stream. In contrast, the periodic operation showed an initial conversion of about 80% which is around 10% lower than that of the steady state operation. The conversion further decreased and became stable after approximately 160 minutes of time on stream. It is obvious that the methane conversion from the periodic operation was inferior to that of the steady state operation over all ranges of reaction time.
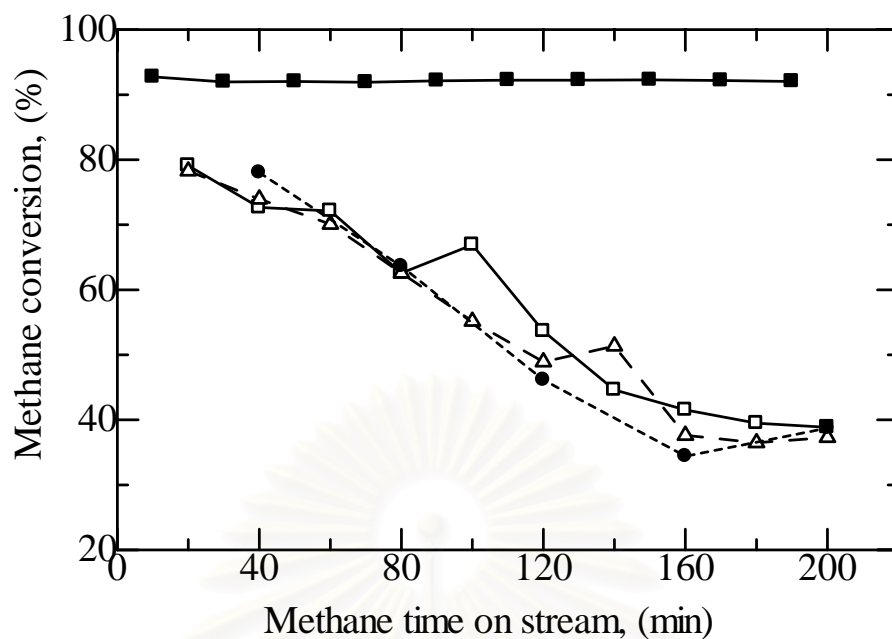
**Figure 5.4** Comparison between steady state operation (■,——); and periodic operation at different cycle period; $(\tau) = 10$ min (□,——); $(\tau) = 20$ min ($\Delta$,— — —); and $\tau = 40$ min (●,- - -); on conversion of methane over $Ni/SiO_2.MgO$ catalyst at 1023 K.
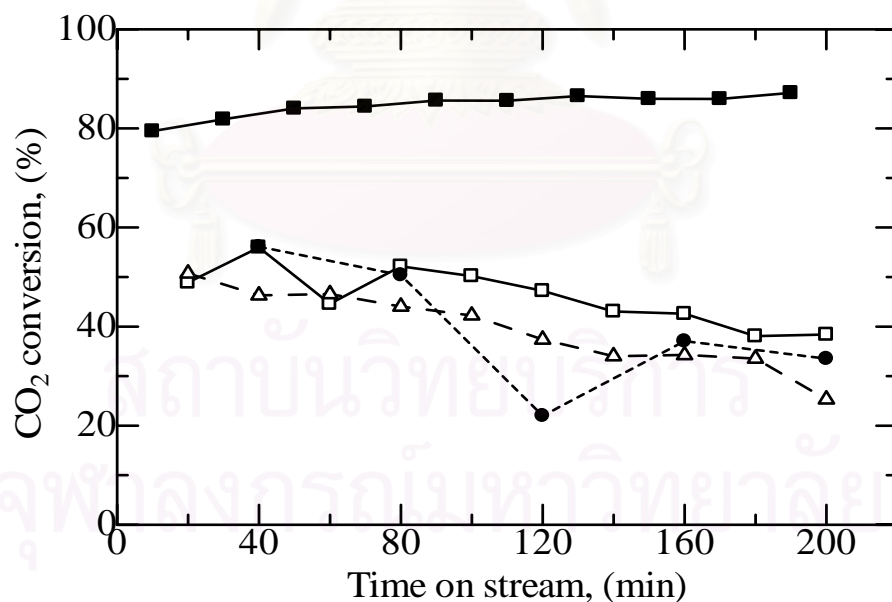


**Figure 5.5** Comparison between steady state operation (■,——); and periodic operation at different cycle period; $(\tau) = 10$ min (□,——); $(\tau) = 20$ min ($\Delta$,— — —); and $\tau = 40$ min (●,- - -); on conversion of $CO_2$ over $Ni/SiO_2.MgO$ catalyst at 1023 K.

The profiles of carbon dioxide conversion with time on stream were shown in Figure 5.5. Similar to the previous results, the carbon dioxide conversion from the steady state operation (85%) did not change with time on stream and the conversion from the periodic operation decreased with increasing repeating cracking/regeneration cycles and then leveled off at high reaction cycles. It was observed when comparing the methane and carbon dioxide conversions for the periodic operation that more coke was accumulated in the catalyst bed along the reaction course due to the difference in their conversion values. However, after 160 minutes of time on stream the rates of coke formation and the coke removal seemed to be equivalent as the conversions of methane and carbon dioxide became comparable at around 40% and consequently the conversions for both reactants no longer changed with reaction time. The profiles of hydrogen yield were shown in Figure 5.6.



**Figure 5.6** Comparison between steady state operation (■,——); and periodic operation at different cycle period; $(\tau) = 10$ min (□,——); $(\tau) = 20$ min ($\Delta$,— — —); and $\tau = 40$ min (●,- - -); on of % Hydrogen yield over Ni/$SiO_2$.MgO catalyst at 1023 K.

It is obvious that the periodic operation offered much lower hydrogen yield than did the steady state operation. The experimental results at different cycle periods (40, 20 and 10 minutes) as also shown in Figures 5.4-5.6 indicate that the cycle period did not pronouncedly affect the reaction performance. At higher cycle period,

although the catalyst may be more deactivated due to the formation of coke during the methane cracking step, more coke can be removed during the regeneration step. Therefore, the average reaction performance may not differ significantly.

Another set of experiments were performed using the same operating conditions as the previous study, except that the temperature was changed from 1023 K to 923 K. Figures 5.7, 5.8 and 5.9 show the profiles of methane conversion, carbon dioxide conversion and hydrogen yield, respectively with time on stream at 923 K.



**Figure 5.7** Comparison between steady state operation (■,——); and periodic operation at different cycle period; ($\tau$) = 10 min (□,——); ($\tau$) = 20 min ($\Delta$,— — —); and $\tau$ = 40 min (●,- - -); on conversion of methane over Ni/SiO$_2$.MgO catalyst at 923 K.

Comparison of the methane conversion between the two temperatures indicates that for the steady state operation, the conversion at 923 K was also stable at 80% which is lower than that of 1023 K (90%). This should be due to the lower reaction rate and less thermodynamic feasibility at lower temperature. However, for the periodic operation it was found that the methane conversion at 923 K was also stable at approximately 60% independent of the cycle period. No indication of activity loss was detected unlike the operation at 1023 K.
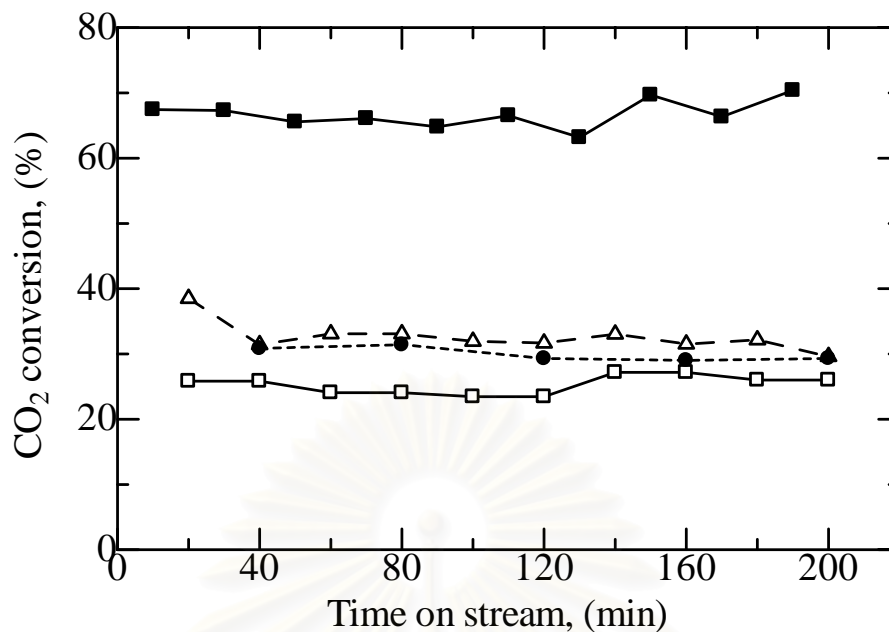
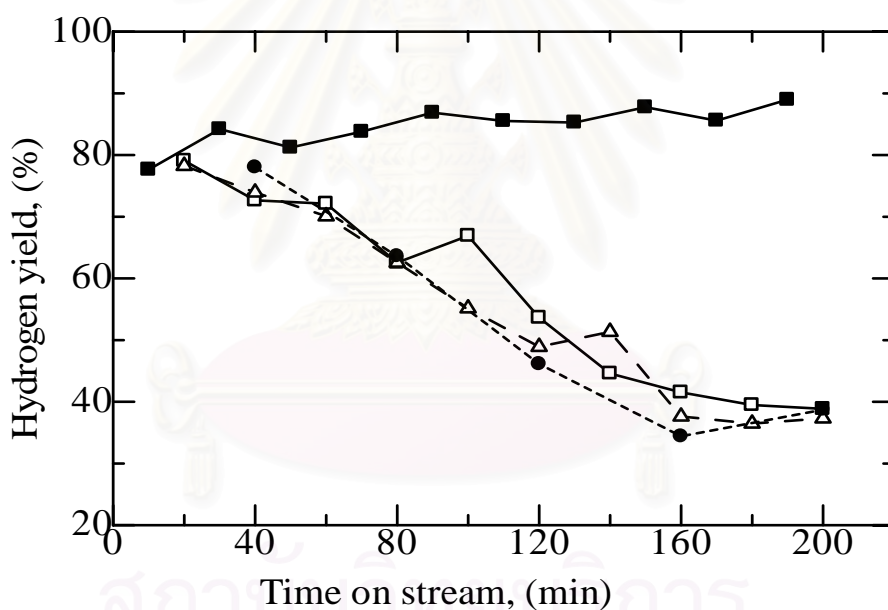**Figure 5.8** Comparison between steady state operation (■,——); and periodic operation at different cycle period; ($\tau$) = 10 min (□,——); ($\tau$) = 20 min ($\Delta$,— — —); and $\tau$ = 40 min (●,- - -); on conversion of $CO_2$ over Ni/$SiO_2$.MgO catalyst at 923 K.
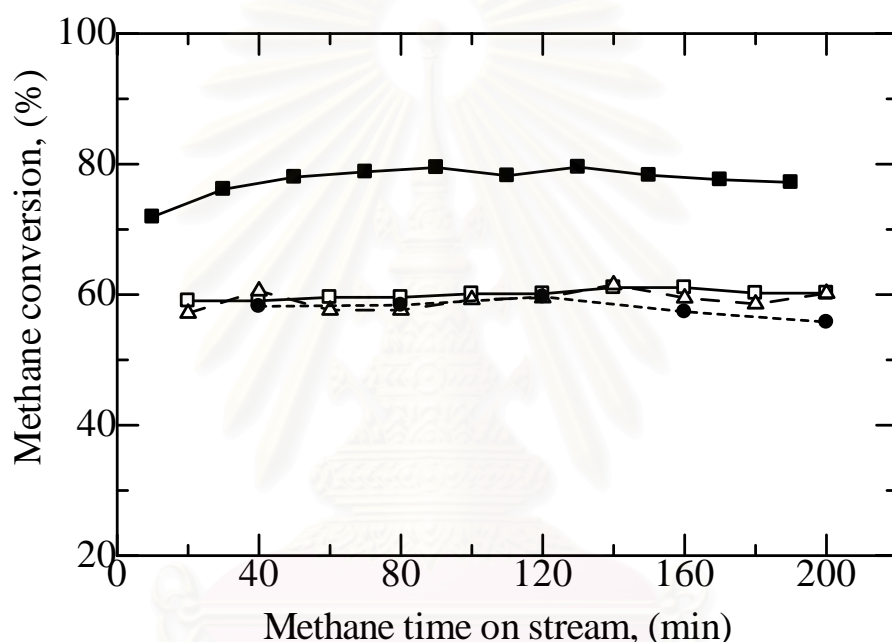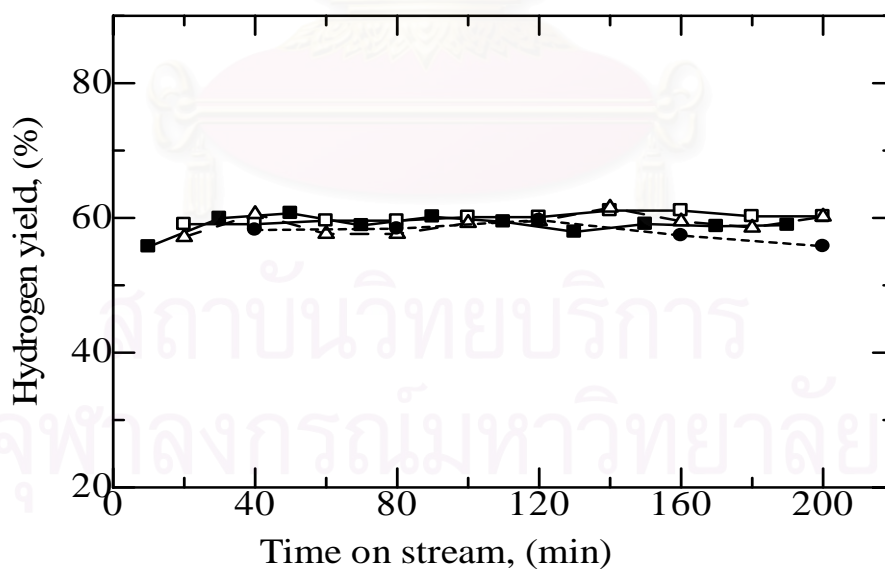


**Figure 5.9** Comparison between steady state operation (■,——); and periodic operation at following cycle time; ($\tau$) = 10 min (□,——); ($\tau$) = 20 min ($\Delta$,— — —); and $\tau$ = 40 min (●,- - -); on of % Hydrogen yield over Ni/$SiO_2$.MgO catalyst at 923 K.

The profiles of carbon dioxide conversion with time on stream for both steady state and periodic operation at 923 K (Figure 5.8) showed stable conversions at approximately 70% and between 25-30%, respectively. Considering the obtained hydrogen yield (Figure 5.9), it was found that the periodic operation provided the hydrogen yield as high as that of the steady state operation, indicating the equivalent performance of the periodic operation at 923 K. It should be noted that the periodic operation also provides another benefit on the separated product streams of hydrogen and carbon monoxide.

Although the periodic operation seemed to become an attractive operation mode at 923 K regarding the equivalent hydrogen yield and stable performance, the comparison between the conversions of methane and carbon dioxide surprisingly indicate that more coke was further accumulated in the catalyst bed after each cracking/regeneration cycle. However, an unusual stable reaction activity throughout the reaction course was observed which is in contrast to the behavior at 1023 K reported earlier. Scanning electron microscopy (SEM) technique was used to observe the difference between catalyst samples that were subjected to 10 cracking/regeneration cycles (cycle period = 20 minutes) with reaction temperature 923 K and 1023 K, as well as a fresh catalyst sample. Both micrographs of the spent catalyst at 923 K (Figure 10d) and 1023 K (Figure 10c) showed the surface to be covered with filamentous carbon, in contrast to the clean surfaces of fresh catalyst (Figures 10a-10b).


(a)


(b)
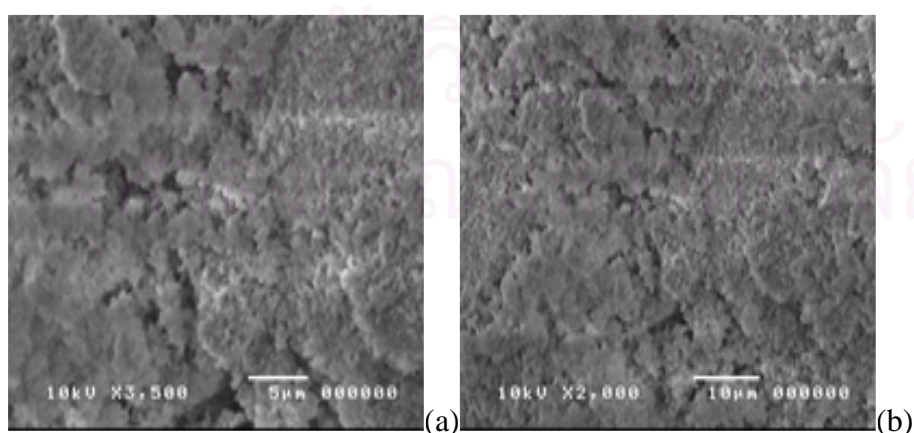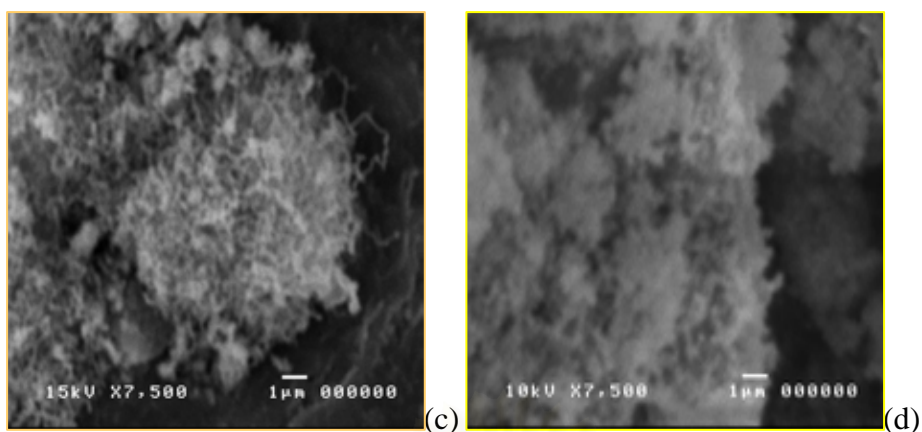
**Figure 5.10** SEM Micrograph of (a) and (b) fresh catalyst, (c) Spent catalyst at 1023 K., and (d) Spent catalyst at 923 K. after 10 successive cracking/regeneration cycles.

In order to understand this dissimilar behavior, an X-ray diffraction technique was chosen to identify the crystal structure of Ni metallic and other metal forms on the catalysts. The characterizations were performed for the spent catalysts obtained after the periodic operation experiments at 923 K (cycle period = 20 minutes) and 1023 K (cycle period = 10 and 20 minutes) with the cycle split ($s$) of 0.5. The measurement of the fresh catalyst was also carried out for comparison.

The XRD patterns shown in Figure 5.11 indicated that nickel contained in the fresh catalyst has crystal structure of NiO (peaks at $2\theta$ = 37.1, 43.1 and 62.7) which would be reduced with hydrogen to convert nickel oxide into the metallic nickel before starting the reaction. It also showed the presence of carbon of graphitic nature evident from the strong peak at $2\theta$ = 26 contaminated in the fresh catalyst sample as well as carbon accumulated in the spent catalysts. Considering the spent catalyst from periodic experiment with cycle period of 20 minutes at 1023 K, the strong peaks of Ni metallic crystallize at $2\theta$ = 44.5, 51.8, and 76.4 were observed with only small intensity of NiO peaks. It was presumed that NiO in the fresh catalyst could be completely reduced to metallic form after Pre-reduction step. For the spent catalysts at lower temperature (923 K), the XRD patterns of spent catalysts from both 10 and 20 minute cycle periods indicated the existence of NiO peaks with lower Ni metallic intensity. It was suggested that NiO could be formed during the cracking/regeneration period and considered to be the active components for cracking period at 923 K.

Therefore, it is evident that the metal active sites involved in the reaction are in different form depending on the operating temperature.
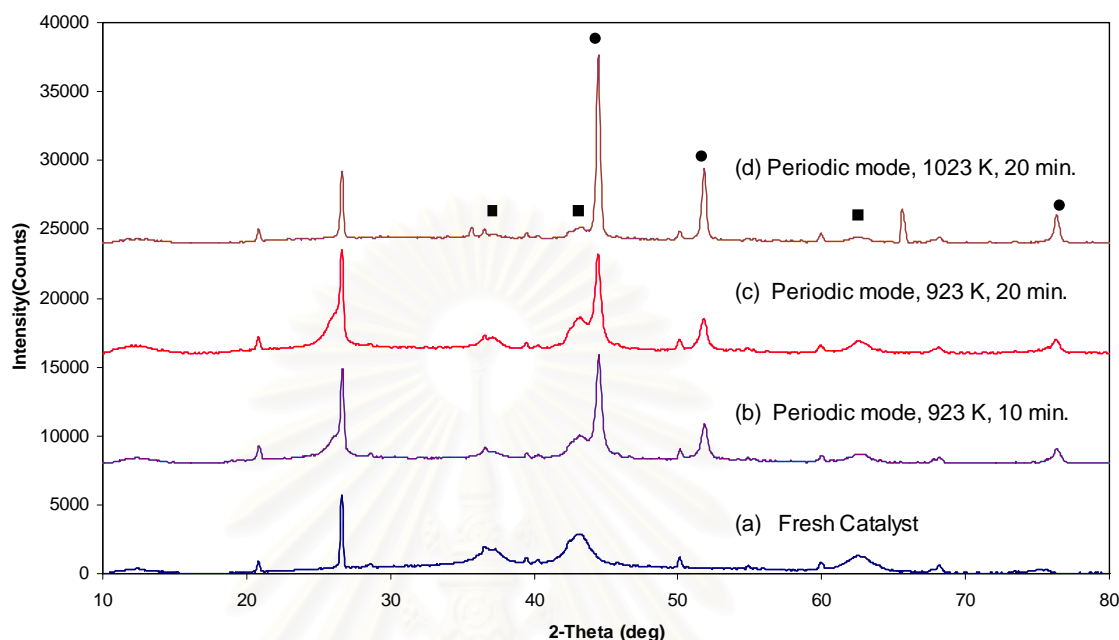


**Figure 5.11** XRD spectra of fresh catalyst and spent catalysts

According to the different operating temperature and form of metal active site, the mechanisms of coke formation are different. Many researchers have suggested that the main type of carbon species which would be formed during the cracking period at high temperature is carbon whisker (Kuijpers et al., 1981; Poirier et al., 1995). In the early stages of the deposition step, deposited carbon filaments could detach small nickel cores from bulk nickel on support. Then, the detached nickel cores which act as a growing core of whisker carbon could still accelerate the rate of carbonaceous deposition and increased their length with time on stream. After switching to the regeneration step, the carbon filaments are burned out with carbon dioxide and the nickel particles fall on the surface. The small nickel particles removed by regeneration may become inactive after next cracking steps (Zhang *et al.*, 1998; Ito *et al.*, 1999). Based on this suggestion, at the reaction temperature of 1023 K, it was described that the rate of methane cracking was higher than the rate of oxidation of carbon deposited with carbon dioxide. Therefore, after each cycle with equal time of cracking and regeneration ($s = 0.5$), the carbonaceous deposit which cannot be

removed during the regeneration step could be accumulated. The growth of new carbon filaments could be terminated as a result of spatial limitations. The type of carbon filament termination included the nickel particle's restriction by the support surface, the arm, and the tip of another carbon filament (Zhang *et al*., 1998). Consequently, the methane conversion decreased with time on stream as clearly shown in Figure 5.1.

A commonly accepted mechanism of filament growth consist of the decomposition of methane at gas-metal interface produced carbon species on the front surface of metal, followed by dissolution of carbon into the metal, diffusion through the particle, precipitation at the metal-support interface, and detaching the metal particle from the support and the forming a filament with an exposed metal at its tip as mentioned above. The rate-determining step of this process is the bulk diffusion of the carbon through the metal particle.

Considering the experimental results at 923 K, as mentioned earlier there was additional accumulation of coke after each cracking/regeneration cycle. This is probably due to the slow rate of the regeneration by carbon dioxide particularly at low operating temperature. However, the catalyst activity still remained constant. This unusual behavior should be due to the differences in mechanisms of the coke formation at low temperature.

The formation of carbon filament was expected to be hindered by the low solubility of carbon in metal particle at low temperature (Kuijpers et al., 1981; Poirier et al., 1995). Moreover, the strong interaction between surface oxygen and metal of NiO existed in periodic operation at 923 K, was suggested to terminate the diffusivity of carbon into the nickel. These should be the cause of the different type of carbon formation at 923 K.

In addition, carbon formed during cracking period on the metal active sites can further move to the catalyst support according to the drain-off phenomena which has been reported in some reaction systems. Drain-off carbon would be more stable, while encapsulated carbon which still located on the metal active sites are more active for oxidation with $CO_2$. Therefore, the coke accumulated on the catalyst could be

completely removed during regeneration period, with stable conversion of $CO_2$. This could be the reason for maintaining methane conversion every repeating cracking period at least within the reaction time of 200 minutes in this study.

In practical operation, it is desired for the periodic operation to keep the coke formation as low as possible to avoid the catalyst deactivation. Therefore, another set of experiments were carried out at 923 K with various values of cycle split (*s*). The cycle period was fixed at 20 minutes and the time-average flow rates of the reactant gases were kept at the same values as described earlier. It is expected that due to the slow rate of catalyst regeneration by carbon dioxide, the increase of regeneration period by lowering the feed flow rate of carbon dioxide (in order to keep the same average carbon dioxide flow rate) should help increase the removal of coke arisen from the methane cracking step and the corresponding reaction performance may be improved. The results for the cycle split (*s*) of 0.25, 0.4 and 0.5 were shown in Figures 5.12 and 5.13. It was found that the decrease of the cycle split did not improve the reaction performance as expected. On the other hand, it slightly lowered both the methane and carbon dioxide conversions. This may be due to the shorter residence time during the methane cracking which caused the lower methane conversion. The decrease of carbon dioxide conversion should be due to the higher effect of mass transfer resistance at low reactant flow rate.
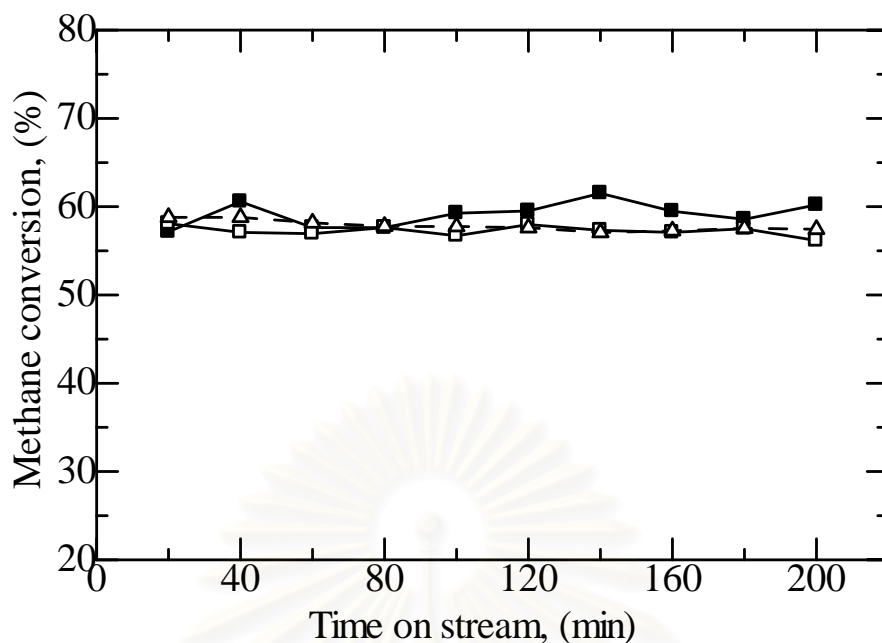
**Figure 5.12** Comparison between periodic operation at different cycle split; s = 0.5 (■,——); s = 0.25 (□,——); and s = 0.4 (Δ,— — —); on conversion of methane over Ni/SiO$_2$.MgO catalyst at 923 K.
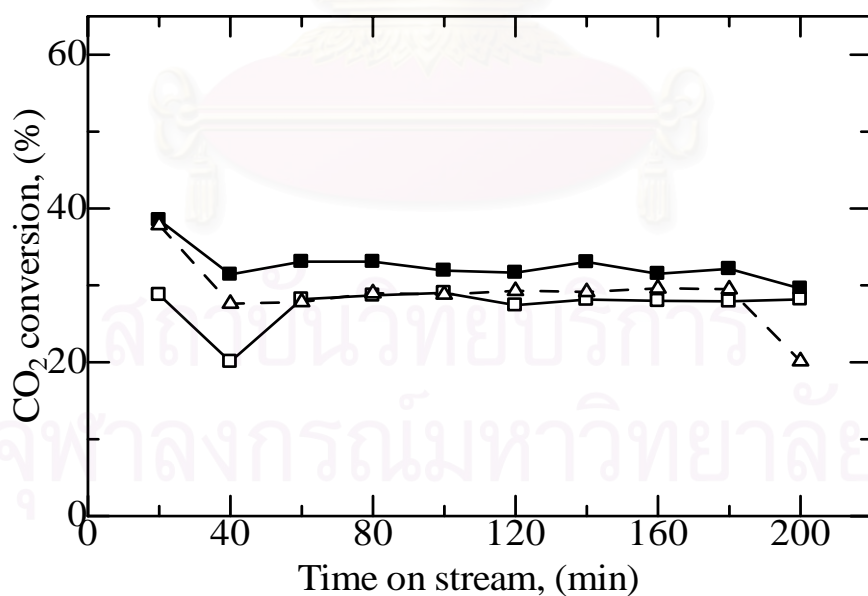


**Figure 5.13** Comparison between periodic operation at different cycle split; s = 0.5 (■,——); s = 0.25  min (□,——); and s = 0.4 (Δ,— — —); on conversion of CO$_2$ over Ni/SiO$_2$.MgO catalyst at 923 K.

# CHAPTER VI
# CONCLUSIONS AND RECOMMENDATION

The experiments were performed to compare the periodic operation data with steady state operation data of the carbon dioxide reforming of methane reaction. The effect of key parameters such as total cycle period, cycle split, and reaction temperature were investigated experimentally to demonstrate the cause-effect relationships in periodic operation. The conclusions of these investigations are shown in Section 6.1. In addition, recommendations for further study are given in Section 6.2.

## 6.1 Conclusions

1. At 1023 K, the methane conversions under periodic operation decreased steeply and became stable after approximately 160 minutes, which was lower than that of the steady state operation over all ranges of reaction time. It is suggested that at high temperature, rate of carbon formation from catalytic cracking of methane is faster than rate of removal of the deposited carbon with carbon dioxide. Carbon whisker could be deposited after repeating each cracking/regeneration period. The loss of catalyst activity was due to the accumulated coke on the catalyst as well as the loss of nickel active site during each regeneration period.

2. At lower temperature (923 K), the methane conversions under both steady state and periodic operation were became inferior to those of 1023 K due to the lower reaction rate and less thermodynamic feasibility at lower temperature. Periodic operation provided the stable methane conversion but with more coke accumulated than that of 1023 K. XRD pattern of spent catalysts indicated that nickel oxide was found to be an active species for cracking reaction. It was suggested that polyaromatic form, not the whisker form of carbon, could be produced at this lower operating temperature with this different metal active site. The catalytic activity was preserved probably

due to the drain-off effect of coke to remove coke from the metal active sites to the catalyst support.

3. No significant effects of cycle period and cycle spilt on the reaction performance were observed at least within the ranges of this study.

4. The advantage of periodic operation over steady state operation for the dry reforming reaction is arisen from separated product streams of hydrogen and carbon monoxide. Moreover, the periodic operation with suitable reaction condition could maintain % yield of hydrogen close to that of the steady state reaction.

**6.2 Recommendations**

From the previous conclusions, the following recommendations for future studies can be proposed.

1. The further investigations should be conducted in order to indicate which types of carbon could be formed in each case of periodic operation. Carbon deposited could have different crystalline structures, morphologies, and reactivities, depending on the specific reaction taking place and the reaction conditions. There are many methods could be used to identify the composition of accumulated coke, including temperature-programmed oxidation (TPO) and Raman spectroscopy (Chen *et al*., 2004; Shamsi *et al*., 2005).

2. Because the ensemble size on the metal surface necessary for the formation of carbon whisker is larger than the ensemble size for other types of carbon formation. The carbon whisker deposition could be reduced by using other types of catalyst which had small ensemble size, such as, Ca (Hou *et al*., 2003), Sn (Hou *et al*., 2004), and Cu (Chen *et al.,* 2004) doped on nickel catalysts. Therefore, the further investigation for improving the efficiency of periodic reaction over these catalysts should be conducted in the future.

3. The other oxidizing gases, such as $H_2O$ (Aiello *et al.*, 2000), are also recommended to study as a reactant gas for the catalyst regeneration reaction as well as using in steam reforming reaction. This reactant is commonly used without converting the metallic nickel into nickel oxide. Moreover, the steam gasification leads to the production of the additional hydrogen with carbon monoxide during reaction period.

4. The periodic operation should be conducted with using wider range of manipulated variables (e.g. several reaction temperature and cycle time) in order to evaluate the best condition for production synthesis gas. In addition, other choice of manipulated variables such as: the time average flow rate; total pressure; and gas feed concentration should be considered.

5. Comparison results between the experiment and the mathematical models are also recommended to investigate the behavior of the system.

# REFERENCES

Aiello, R., Fiscus, J.E., Loye, H-C. and Amiridis, M.D Hydrogen production via the direct cracking of methane over $Ni/SiO_2$: catalyst deactivation and regeneration *App. Cat. A. Gen.*, 2000, **192**, 227–234.

Asami, K., Li, X., Fujimoto, K., Koyama, Y., Sakurama, A., Kometani, N. and Yonezawa, Y $CO_2$ reforming of $CH_4$ over ceria-supported metal catalysts Catal. Today., 2003, **84**, 27-31.

Basini, L., Marchionna, M., Rossini, S. and Sanfilippo, D Catalytic system and process for producing synthesis gas by reforming light hydrocarbons with $CO_2$ *GB Patent No. 2*, 1991 ,**240**, 284.

Chanchlani, K.G., Hudgins, R.R. and Silveston, P.L Methanol synthesis from H2, CO, and C0_2 over Cu/ZnO catalysts *J. of Cat.*, 2003, **136**, 59-75.

Chen, H., Wang, C., Yu, C., Tseng, L. and Liao, P Carbon dioxide reforming of methane reaction catalyzed by stable nickel copper catalysts *Catal .Today.*, 2004, **97**, 173–180.

Edwards, J.H. and Maitra, A.M The chemistry of methane reforming with carbon dioxide and its current and potential applications *Fuel Proc Tech.*, 1995, **42**, 269-289.

Ermakova, M.A. and Ermakov, D.Yu $Ni/SiO_2$ and $Fe/SiO_2$ catalysts for production of hydrogen and filamentous carbon via methane decomposition *Cat Today*, 2002, **77**,225–235.

Fraenkel, D., Levitan, R. and Levy, M A solar thermochemical pipe based on the $CO_2$ : $CH_4$ (1: 1) system *Int. J. Hydrogen Energy.*, 1986, **11,** 267-277.

Goldwasser, M.R., Rivas M.E., Pietri, E., Pérez-Zurita, M.J., Cubeiro, M.L., Gingembre, L., Leclercq, L. and Leclercq, G Perovskites as catalysts precursors: $CO_2$ reforming of $CH_4$ on $Ln_{1.x}Ca_xRu_{0.8}Ni_{0.2}O_3$ (Ln = La, Sm, Nd) *App. Cat. A. Gen.*, 2003, **255**, 45-57.

Gustafson, B.L. and Walden, J.V Conversion of carbon dioxide to carbon monoxide *US Patent No $068,057*, 1991.

Hou, Z.,Yokot, O., Tanaka, T. and Yashima, T Characterization of Ca-promoted $Ni/\alpha-Al_2O_3$ catalyst for $CH_4$ reforming with $CO_2$ *App. Cat. A. Gen.*, 2003, **253**, 381-387.

Hou, Z.,Yokot, O., Tanaka, T. and Yashima, T  Surface properties of a coke-free Sn doped nickel catalyst for the $CO_2$ reforming of methane  *App. Surf. Sci.*, 2004, **xxx** ,xxx–xxx.

Ito, M., Tagawa T. and Goto, S Suppression of carbonaceous depositions on nickel catalyst for the carbon dioxide reforming of methane  *App. Cat. A. Gen.*, 1999, **1177**, 15-23.

Ito, M., Tagawa, T. and Goto, S Partial oxidation of methane on supported nickel catalysts  *J. Chem. Eng. Jpn.*, 1999, **32**, 274-279.

Jing, Q., Lou, H., Mo, L., Fei, J. and Zheng, X  Combination of $CO_2$ reforming and partial oxidation of methane over $Ni/BaO-SiO_2$ catalysts to produce low $H_2/CO$ ratio syngas using a fluidized bed reactor  *J. of Mol. Cat. A. Chem.*, 2004, **212**, 211–217.

Juan-Juan, J., Rom.n-Mart.ýnez, M.C. and Illán-Gómez, M.J  Catalytic activity and characterization of $Ni/Al_2O_3$ and $NiK/ Al_2O_3$ catalysts for $CO_2$ methane reforming  *App. Cat. A. Gen.*, 2004, **264**, 169–174.

Lee, S., Cho, W., Ju, W., Cho, B., Lee, Y. and Baek, Y  Tri-reforming of $CH_4$ using $CO_2$ for production of synthesis gas to dimethyl ether   *Catal. Today.*, 2003, **87**, 133-137.

Masai, M., Kado, H., Miyake, A., Nishiyama, S. and Tsuruya, S., "Methane reforming by carbon dioxide and steam over supported Pd, Pt and Rh catalysts.", *Stud. Surf. Sci. Catal.*, 1988, **36**, 67-71.

Matsumura,Y. and Nakamori, T  Steam reforming of methane over nickel catalysts at low reaction temperature *App. Cat. A. Gen.*, 2004, **258**, 107-114.

Monnerat, B., Kiwi-Minsker, L. and Renken, A  Hydrogen production by catalytic cracking of methane over nickel gauze under periodic reactor operation *Chem. Eng. Sci.*, 2001, **56**, 633-639.

Perera, J.S.H.Q., Couves, J.W., Sankar, G. and Thomas, J.M  The catalytic activity of Ru and Ir supported on $Eu_2O_3$ for the reaction, $CO_2 + CH_4 = 2H_2 + 2CO$: a viable solar-thermal energy system  *Catal. Lett., 1991,* **11**, 219-225.

Rambeau, G. and Amariglio, H  Improvement of the catalytic performance of a ruthenium powder in ammonia synthesis by the use of a cyclic procedure *App. Cat.*, 1981, **1**, 107-114.

Richardson, J.T. and Paripatyadar, S.A  Carbon dioxide reforming of methane with supported rhodium *App. Cat.*, 1990, **61**, 293-309.

Shamsi, A., Baltrus, J. P. and Spivey, J.J Characterization of coke deposited on Pt/alumina catalyst during reforming of liquid hydrocarbons *App. Cat. A. Gen.*, 2005, **293**, 145–152.

Silveston, P., Hudgins, R.R. and Renken, A  Periodic operation of catalytic reactors - introduction and overview  *Catal. Today.*, 1995, **25**, 91-112.

Snoeck, J.W., Froment,  G. F. and  Fowlesz, M  Filamentous Carbon Formation and Gasification: Thermodynamics, Driving Force, Nucleation, and Steady-State Growth  *J. of Cat.*, 1997, **169**, 240–249.

Solymosi, F  The bonding, structure and reactions of $CO_2$ adsorbed on clean and promoted metal surfaces *J. Mol. Catal.*, 1991.  **65**: 3377358.

Solymosi, F., Erdohelyi, A. and Cserenyi, J  A comparative study on the activation and reactions of $CH_4$ on supported metals  *Catal. Lett.*, 1992, **16**, 399-405.

Solymosi, F., Erdohelyi, A. and Cserenyi, J  Activation of $CH_4$ and its reaction with $CO_2$ over supported Rh catalysts  *J. Catal.*, 1993, **141**,  287-299.

Souza, M. M. V. M. and Schmal, Martin  Combination of carbon dioxide reforming and partial oxidation of methane over supported platinum catalysts  *App. Cat. A. Gen.*, 2003, **255**, 83-92.

Takano, A., Tagawa, T. and Goto, S  Carbon deposition on supported nickel catalysts for carbon dioxide reforming of methane  *Sekiyu Gakkaishi.*, 1996, **39**, 144-149.

Takano, A., Tagawa, T. and Goto, S   Carbon dioxide reforming of methane on supported nickel catalysts *J. Chem. Eng. Jpn.*, 1994, **27**, 727 -731.

Tsang, S.C., Claridge, J.B. and Green, M.L.H  Recent advances in the conversion of methane to synthesis gas *Catal. Today.*, 1995, **23**, 3-15.

Uchijima, T., Nakamura, J., Sato, K., Aikawa, K., Kubushiro, K. and Kunimori, K  Production of synthesis gas by partial oxidation of methane and reforming of methane wtih carbon dioxide *Poster paper 18 presented at the Natural Gas Conversion Symp., Sydney*, 1993, July 49.

Zhang, T. and Amiridis, M.D  Hydrogen production via the direct cracking of methane over silica-supported nickel catalysts  *App. Cat. A. Gen.*, 1998, **167**, 161–172.

# APPENDICES

# APPENDIX A
# CALCULATION

The catalyst performance for the carbon dioxide reforming of methane in both steady state operation and periodic operation was evaluated in many ways.

### Conversion of methane and carbon dioxide

Activity of the catalyst performed in term of methane conversion. In case of steady state reaction, methane conversion was defined as mole flow rate of methane reacted during the reaction period ($F_{CH_4, reacted}$), with respect to inlet mole flow rate of methane in feed passed through reactor during the reaction period ($F_{CH_4, in}$)

$$CH_4 \ Conversion \quad (\%) \quad = \quad 100 \times \frac{(F_{CH_4, reacted})}{(F_{CH_4, in})} \tag{A1}$$

Where flow rate of methane reacted can be obtained from a difference between inlet flow rate ($F_{CH4, in}$ = 12.5 cc/min.) and outlet flow rate of methane ($F_{CH4, out}$). Outlet mole flow rate of methane can be calculated from overall flow rate of gas outlet measured from bubble flow meter ($F_{total, out}$), multiplied with mole ratio of methane with respect to total mole of all outlet gaseous products. ($F_{total, out}$).

$$F_{CH_4, reacted} \quad = \quad (12.5 - F_{total, out} \times (\frac{mole \ of \ CH_4}{mole \ of \ total \ gas \ product})) \tag{A2}$$

Composition each gaseous product in total gas product (which could be consisted of $CH_4$, $CO_2$, $H_2$, and CO) could be calculated with the calibration curve from Figure B.1-B.4, Appendix B., i.e.,

$$mole \ of \ CO \quad = \quad ((Area \ of \ CO \ from \ \text{int} egrator \ plot \ on \ GC - 8A) \times (5 \times 10^{-11}))$$

$$\tag{A3}$$

$$mole \ of \ CO_2 \ = \ ((Area \ of \ CO_2 \ from \ \mathrm{integrator} \ plot \ on \ GC-8A) \times (7 \times 10^{-11}))$$

(A4)

$$mole \ of \ CH_4 \ = \ ((Area \ of \ CH_4 \ from \ \mathrm{integrator} \ plot \ on \ GC-8A) \times (2 \times 10^{-11}))$$

(A5)

$$mole \ of \ H_2 \ = \ ((Area \ of \ H_2 \ from \ \mathrm{integrator} \ plot \ on \ GC-8A) \times (5 \times 10^{-12}))$$

(A6)

Conversion of carbon dioxide also could be obtained in a similar way as calculation of methane conversion.

$$CO_2 \ Conversion \quad (\%) \ = \ 100 \times \frac{(F_{CO_2,reacted})}{(F_{CO_2,in})}$$

(A7)

In case of periodic operation, the main reaction in the reactor could be separated to catalytic cracking of methane ($CH_4 \rightarrow C + 2H_2$) and catalyst regeneration with carbon dioxide ($CO_2 + C \rightarrow 2CO$). A mixture of reactant and product gas from cracking period ($CH_4$, $H_2$) and regeneration period ($CO_2$, $CO$) would be collected with the same sampling bag after finished each cycle.

The sample would be taken for analyzing of gas composition from sampling bag. The conversion of methane in cracking period and conversion of carbon dioxide in regeneration period for periodic mode could be gained as followed;

$$CH_4 \ Conversion \ (Periodic) - (\%) \ = \ 100 \times \frac{(\frac{mole \ of \ H_2 \ outlet}{mole \ of \ CH_4 \ outlet})}{(2 + \frac{mole \ of \ H_2 \ outlet}{mole \ of \ CH_4 \ outlet})}$$

(A8)

$$CO_2 \ Conversion \ (Periodic) - (\%) \ = \ 100 \times \frac{(\frac{mole \ of \ CO \ outlet}{mole \ of \ CO_2 \ outlet})}{(2 + \frac{mole \ of \ CO \ outlet}{mole \ of \ CO_2 \ outlet})}$$

(A9)

**Hydrogen selectivity**

Hydrogen selectivity of product gas is also used to the compare the performance of steady state with periodic operation. Because of only cracking reaction was conducted for period operation to generate hydrogen product, selectivity of $H_2$ was considered to be 100%. On the other hand, Hydrogen selectivity could be changed due to reverse water-gas shift reaction, which is thermodynamically feasible for carbon dioxide reforming of methane. Therefore, hydrogen selectivity could be computed by (Eq. (A10));

$$Hydrogen\ selectivity\ (\%) \ = \ 100 \times \frac{(F_{H_2,out})}{(2 \times F_{CH_4,reacted})} \qquad (A10)$$

While hydrogen flow rate could be obtained with similar method as methane flow rate.

$$F_{H_2,out} \ = \ (F_{total,out} \times (\frac{mole\ of\ H_2}{mole\ of\ total\ gas\ product})) \qquad (A11)$$

**%Yield of hydrogen**

In addition, % yield of hydrogen is also used to show the performance for both steady state and periodic operation. It was defined as selectivity of hydrogen product, multiplied with conversion of methane reactant.

$$\%Yield\ of\ hydrogen \ = \ (Hydrogen\ selectivity \times Methane\ conversion) \qquad (A12)$$

# APPENDIX B
# CALIBRATION CURVES

This appendix shows the calibration curves for calculation of composition of reactant and products in the carbon dioxide reforming of methane reaction. The reactants are carbon dioxide and methane. The products are synthesis gas, containing carbon monoxide and hydrogen.

The Gas chromatography Shimadzu model 8A with a thermal conductivity detector (TCD), was used for analyzing the concentration of all reactants and products by using Molecular sieve 5A column and Porapak-Q column, respectively. Conditions used in for GC analyzing are illustrated in Table B.1.

Mole of reagent in y-axis and area reported by gas chromatography in x-axis are exhibited in the curves. The calibration curves of carbon monoxide, carbon dioxide, methane, and hydrogen are shown in the following figures.

**Table B.1** Conditions used in Shimadzu model GC-8A

| Parameters | Condition (Shimadzu GC-8A) |
|---|---|
| Width | 5 |
| Slope | 50 |
| Drift | 0 |
| Min. area | 10 |
| T.DBL | 0 |
| Stop time | 30 |
| Atten | 5 |
| Speed | 2 |
| Method | 41 |
| Format | 1 |
| SPL.WT | 100 |
| IS.WT | 1 |
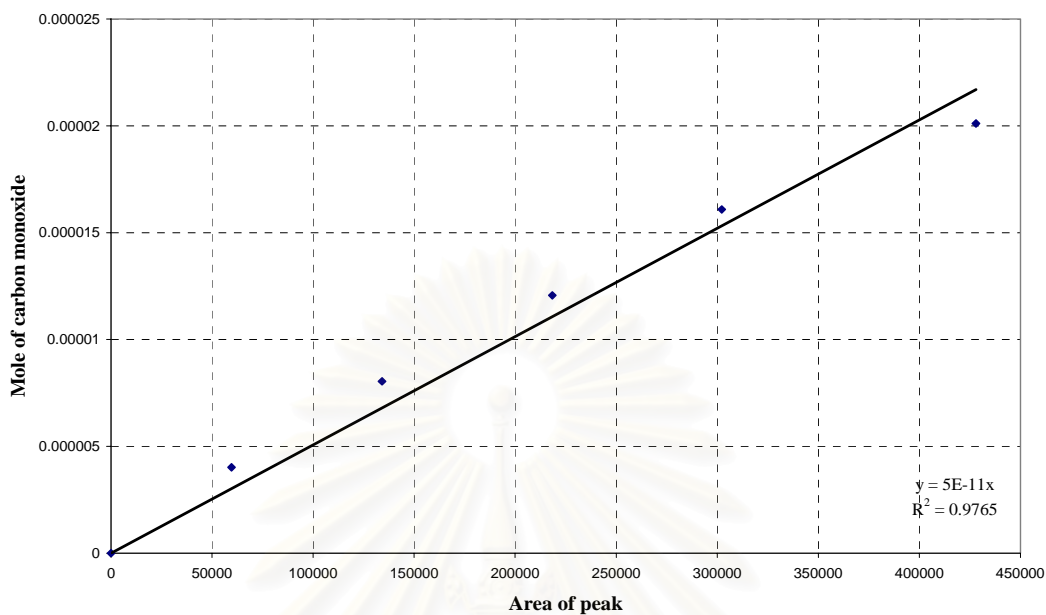
**Figure B.1** The calibration curve of carbon monoxide (Peak time was analyzed at 11 min by using Molecular Sieve 5A GC column.)
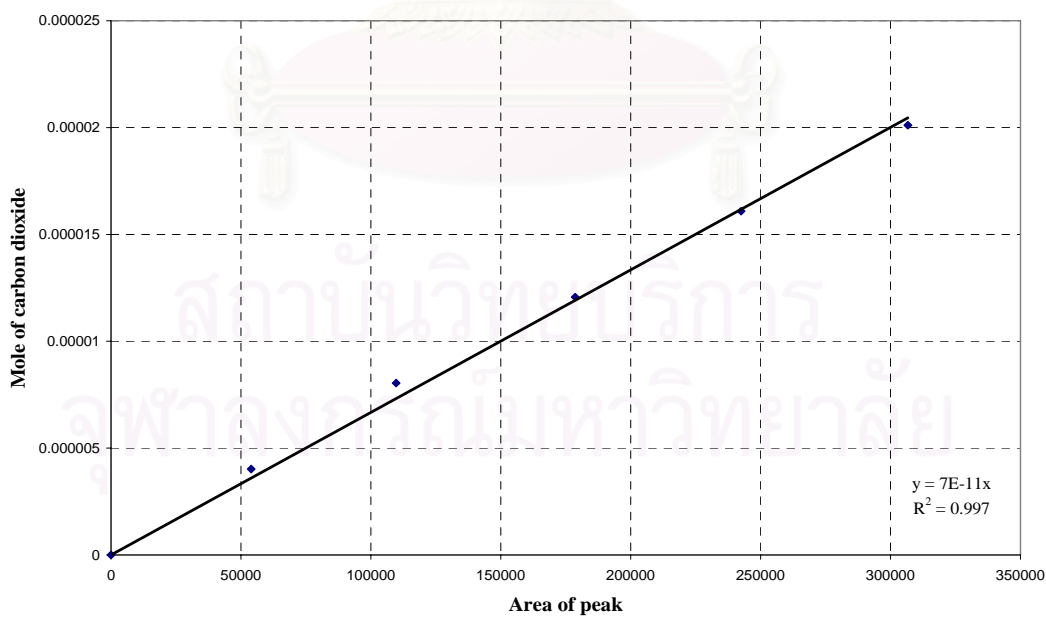


**Figure B.2** The calibration curve of carbon dioxide (Peak time was analyzed at 1.4 min by using Porapak-Q GC column.)
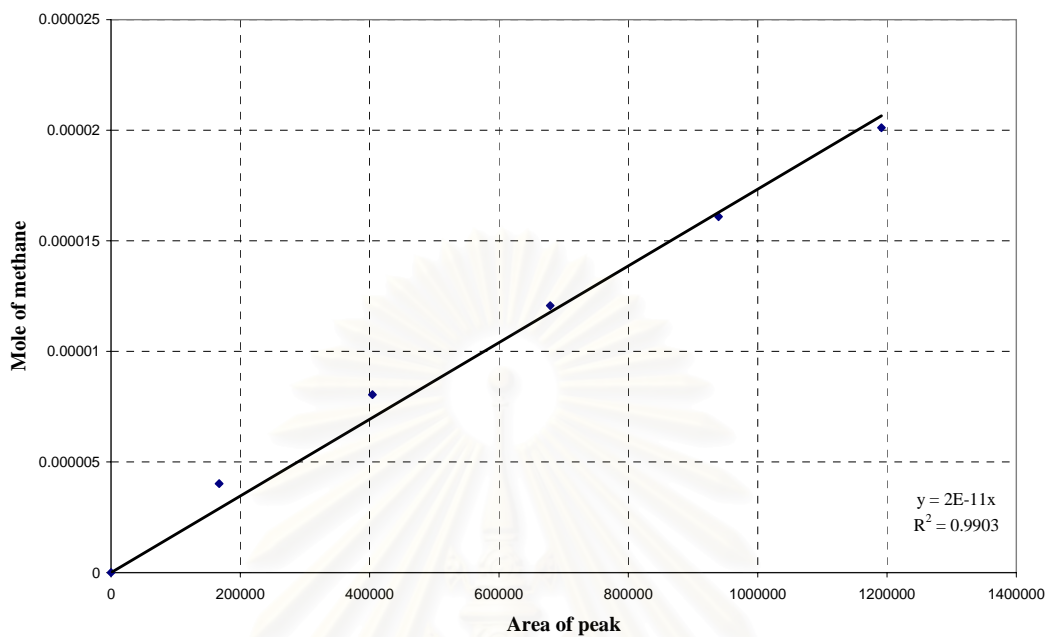
**Figure B.3** The calibration curve of methane (Peak time was analyzed at 4.5 min by using Molecular Sieve 5A GC column.)
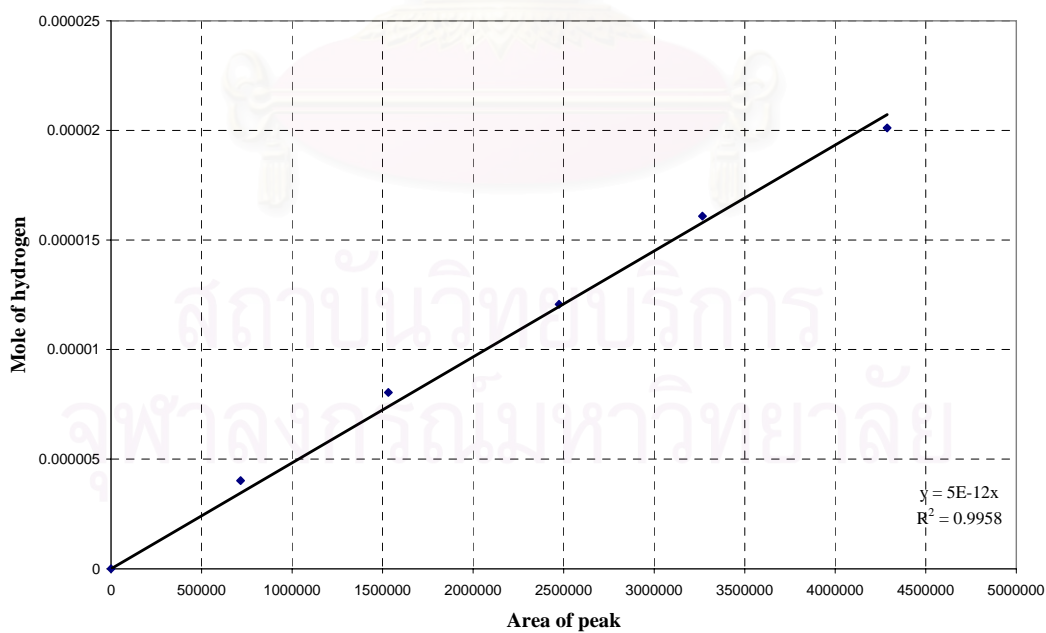


**Figure B.4** The calibration curve of hydrogen (Peak time was analyzed at 0.9 min by using Molecular Sieve 5A GC column.)

# APPENDIX C
# DATA OF EXPERIMENTS

**Table C1**  Data of Figure 5.1

| time on stream (min) | Pressure drop (Pa) | Methane conversion (%) |
|---|---|---|
| 0.00 | 44.61 | |
| 3.00 | 53.54 | 72.34 |
| 5.00 | 44.61 | 72.27 |
| 15.00 | 44.61 | 64.33 |
| 25.00 | 49.08 | 50.80 |
| 35.00 | 53.54 | 33.10 |
| 45.00 | 58.00 | 17.07 |
| 55.00 | 62.46 | 15.16 |
| 65.00 | 62.46 | 13.42 |
| 75.00 | 62.46 | 12.65 |
| 85.00 | 62.46 | 11.73 |
| 95.00 | 62.46 | 11.00 |
| 105.00 | 62.46 | 10.13 |
| 115.00 | 62.46 | 9.48 |
| 125.00 | 62.46 | 9.27 |
| 145.00 | 62.46 | 8.31 |
| 165.00 | 62.46 | 7.77 |
| 185.00 | 62.46 | 7.13 |
| 225.00 | 62.46 | 6.61 |

**Table C2** Data of Figure 5.3

| Time on stream (min) | $CO_2$ conversion (%) |
|---|---|
| 0 | |
| 3 | 54.48 |
| 15 | 52.01 |
| 25 | 31.14 |
| 30 | 3.61 |
| 35 | 1.18 |
| 50 | 0.87 |
| 60 | 0.79 |

| Time on stream (min) | Pressure drop (Pa) |
|---|---|
| 0 | 62.46 |
| 5 | 53.54 |
| 10 | 53.54 |
| 15 | 44.61 |
| 20 | 35.69 |
| 25 | 26.77 |
| 35 | 26.77 |
| 40 | 26.77 |
| 45 | 17.85 |
| 50 | 17.85 |
| 60 | 17.85 |

**Table C3** Data of Figure 5.4

| Steady state | | Periodic operation | Cycle period 40 min. |
|---|---|---|---|
| Time on stream (min) | Methane conversion (%) | Time on stream (min) | Methane conversion (%) |
| 0 | | 0 | |
| 10 | 92.74 | 40 | 78.02 |
| 30 | 91.96 | 80 | 63.63 |
| 50 | 92.02 | 120 | 46.13 |
| 70 | 91.90 | 160 | 34.41 |
| 90 | 92.14 | 200 | 38.73 |
| 110 | 92.24 | | |
| 130 | 92.22 | | |
| 150 | 92.27 | | |
| 170 | 92.20 | | |
| 190 | 92.04 | | |

**Table C3** Data of Figure 5.4 (cont.)

| Periodic operation | Cycle period 20 min. | Cycle period 40 min. |
|---|---|---|
| Time on stream (min) | Methane conversion (%) | Methane conversion (%) |
| 0 | | |
| 20 | 79.09 | 78.26 |
| 40 | 72.66 | 73.95 |
| 60 | 72.12 | 70.08 |
| 80 | 62.58 | 62.58 |
| 100 | 66.91 | 55.16 |
| 120 | 53.65 | 48.92 |
| 140 | 44.60 | 51.35 |
| 160 | 41.53 | 37.62 |
| 180 | 39.49 | 36.48 |
| 200 | 38.85 | 37.30 |

**Table C4** Data of Figure 5.5

| Steady state | | Periodic operation | Cycle period 40 min. |
|---|---|---|---|
| Time on stream (min) | $CO_2$ conversion (%) | Time on stream (min) | $CO_2$ conversion (%) |
| 0 | | 0 | |
| 10 | 75.52 | 40 | 56.12 |
| 30 | 81.84 | 80 | 50.40 |
| 50 | 84.04 | 120 | 22.00 |
| 70 | 84.45 | 160 | 37.06 |
| 90 | 85.63 | 200 | 33.50 |
| 110 | 85.59 | | |
| 130 | 86.52 | | |
| 150 | 85.98 | | |
| 170 | 85.95 | | |
| 190 | 87.18 | | |

**Table C4** Data of Figure 5.5 (cont.)

| Periodic operation | Cycle period 10 min. | Cycle period 20 min. |
|---|---|---|
| Time on stream (min) | $CO_2$ conversion (%) | $CO_2$ conversion (%) |
| 0 | | |
| 20 | 48.90 | 50.73 |
| 40 | 55.99 | 46.31 |
| 60 | 44.59 | 46.58 |
| 80 | 52.15 | 44.05 |
| 100 | 50.20 | 42.25 |
| 120 | 47.22 | 37.39 |
| 140 | 43.05 | 34.03 |
| 160 | 42.59 | 34.27 |
| 180 | 38.08 | 33.55 |
| 200 | 38.38 | 25.32 |

**Table C5** Data of Figure 5.6

| Steady state | | Periodic operation | Cycle period 40 min. |
|---|---|---|---|
| Time on stream (min) | %Yield $H_2$ | Time on stream (min) | %Yield $H_2$ |
| 0 | | 0 | |
| 10 | 77.66 | 40 | 78.02 |
| 30 | 84.22 | 80 | 63.63 |
| 50 | 81.22 | 120 | 46.13 |
| 70 | 83.78 | 160 | 34.41 |
| 90 | 86.87 | 200 | 38.73 |
| 110 | 85.53 | | |
| 130 | 85.28 | | |
| 150 | 87.76 | | |
| 170 | 85.59 | | |
| 190 | 88.97 | | |

**Table C5** Data of Figure 5.6 (cont.)

| Periodic operation | Cycle period 10 min. | Cycle period 20 min. |
|---|---|---|
| Time on stream (min) | % Yield $H_2$ | % Yield $H_2$ |
| 0 | | |
| 20 | 79.09 | 78.26 |
| 40 | 72.66 | 73.95 |
| 60 | 72.12 | 70.08 |
| 80 | 62.58 | 62.58 |
| 100 | 66.91 | 55.16 |
| 120 | 53.65 | 48.92 |
| 140 | 44.60 | 51.35 |
| 160 | 41.53 | 37.62 |
| 180 | 39.49 | 36.48 |
| 200 | 38.85 | 37.30 |

**Table C6** Data of Figure 5.7

| Steady state | | Periodic operation | Cycle period 40 min. |
|---|---|---|---|
| Time on stream (min) | Methane conversion (%) | Time on stream (min) | Methane conversion (%) |
| 0 | | 0 | |
| 10 | 71.92 | 40 | 58.21 |
| 30 | 76.15 | 80 | 58.40 |
| 50 | 77.99 | 120 | 59.67 |
| 70 | 78.80 | 160 | 57.38 |
| 90 | 79.48 | 200 | 55.79 |
| 110 | 78.22 | | |
| 130 | 79.55 | | |
| 150 | 78.29 | | |
| 170 | 77.62 | | |
| 190 | 77.19 | | |

**Table C6** Data of Figure 5.7 (cont.)

| Periodic operation | Cycle period 10 min. | Cycle period 20 min. |
|---|---|---|
| Time on stream (min) | Methane conversion (%) | Methane conversion (%) |
| 0 | | |
| 20 | 59.06 | 57.16 |
| 40 | 59.06 | 60.58 |
| 60 | 59.58 | 57.62 |
| 80 | 59.58 | 57.62 |
| 100 | 60.13 | 59.26 |
| 120 | 60.13 | 59.51 |
| 140 | 61.09 | 61.52 |
| 160 | 61.09 | 59.49 |
| 180 | 60.23 | 58.57 |
| 200 | 60.23 | 60.20 |

**Table C7** Data of Figure 5.8

| Steady state | | Periodic operation | Cycle period 40 min. |
|---|---|---|---|
| Time on stream (min) | $CO_2$ conversion (%) | Time on stream (min) | $CO_2$ conversion (%) |
| 0 | | 0 | |
| 10 | 67.44 | 40 | 30.86 |
| 30 | 67.30 | 80 | 31.42 |
| 50 | 65.55 | 120 | 29.30 |
| 70 | 66.08 | 160 | 29.01 |
| 90 | 64.80 | 200 | 29.32 |
| 110 | 66.51 | | |
| 130 | 63.17 | | |
| 150 | 69.67 | | |
| 170 | 66.34 | | |
| 190 | 70.38 | | |

**Table C7** Data of Figure 5.8 (cont.)

| Periodic operation | Cycle period 10 min. | Cycle period 20 min. |
|---|---|---|
| Time on stream (min) | $CO_2$ conversion (%) | $CO_2$ conversion (%) |
| 0 | | |
| 20 | 25.82 | 38.51 |
| 40 | 25.82 | 31.42 |
| 60 | 24.06 | 33.09 |
| 80 | 24.06 | 33.09 |
| 100 | 23.45 | 31.94 |
| 120 | 23.45 | 31.67 |
| 140 | 27.18 | 33.05 |
| 160 | 27.18 | 31.52 |
| 180 | 26.00 | 32.16 |
| 200 | 26.00 | 29.60 |

**Table C8** Data of Figure 5.9

| Steady state | | Periodic operation | Cycle period 40 min. |
|---|---|---|---|
| Time on stream (min) | %Yield $H_2$ | Time on stream (min) | %Yield $H_2$ |
| 0 | | 0 | |
| 10 | 55.73 | 40 | 58.21 |
| 30 | 59.95 | 80 | 58.40 |
| 50 | 60.68 | 120 | 59.67 |
| 70 | 58.88 | 160 | 57.38 |
| 90 | 60.17 | 200 | 55.79 |
| 110 | 59.43 | | |
| 130 | 57.93 | | |
| 150 | 59.08 | | |
| 170 | 58.75 | | |
| 190 | 58.93 | | |

**Table C8** Data of Figure 5.9 (cont.)

| Periodic operation | Cycle period 10 min. | Cycle period 20 min. |
|---|---|---|
| Time on stream (min) | % Yield $H_2$ | % Yield $H_2$ |
| 0 | | |
| 20 | 59.06 | 57.16 |
| 40 | 59.06 | 60.58 |
| 60 | 59.58 | 57.62 |
| 80 | 59.58 | 57.62 |
| 100 | 60.13 | 59.26 |
| 120 | 60.13 | 59.51 |
| 140 | 61.09 | 61.52 |
| 160 | 61.09 | 59.49 |
| 180 | 60.23 | 58.57 |
| 200 | 60.23 | 60.20 |

**Table C9** Data of Figure 5.12

| Time on stream (min) | $CH_4$ conversion (%) | | |
|---|---|---|---|
| | Cycle period 10 min. | Cycle period 20 min. | Cycle period 40 min. |
| 0 | | | |
| 20 | 57.16 | 58.09 | 58.80 |
| 40 | 60.58 | 57.08 | 58.80 |
| 60 | 57.62 | 56.96 | 58.17 |
| 80 | 57.62 | 57.63 | 57.78 |
| 100 | 59.26 | 56.71 | 57.75 |
| 120 | 59.51 | 57.99 | 57.62 |
| 140 | 61.52 | 57.32 | 57.07 |
| 160 | 59.49 | 57.09 | 57.27 |
| 180 | 58.57 | 57.50 | 57.55 |
| 200 | 60.20 | 56.16 | 57.44 |

**Table C10**  Data of Figure 5.13

| Time on stream (min) | CO$_2$ conversion (%) | | |
|---|---|---|---|
| | Cycle period 10 min. | Cycle period 20 min. | Cycle period 40 min. |
| 0 | | | |
| 20 | 38.51 | 28.79 | 37.87 |
| 40 | 31.42 | 20.09 | 27.63 |
| 60 | 33.09 | 28.21 | 27.86 |
| 80 | 33.09 | 28.71 | 28.99 |
| 100 | 31.94 | 29.04 | 28.82 |
| 120 | 31.67 | 27.44 | 29.30 |
| 140 | 33.05 | 28.16 | 29.15 |
| 160 | 31.52 | 28.00 | 29.62 |
| 180 | 32.16 | 27.93 | 29.51 |
| 200 | 29.60 | 28.19 | 20.15 |

# VITA

Mr. Eakkapon Promaros was born on April 19, 1982 in Bangkok, Thailand. He finished high school from Mahidol Wittayanusorn School, Nakornpathom in 2001, and received the bachelor's degree in Chemical Engineering from Faculty of Engineering, Chulalongkorn University in 2004. He continued his master's study at Chulalongkorn University in June, 2004.